Swfit UVOT

MULLARD SPACE SCIENCE LABORATORY
UNIVERSITY COLLEGE LONDON
Author: H. Kawakami

Detector System Design II

<< Coincidence for a point source object >>

Document Number: Swift-UVOT/MSSL/TN/006.01 **24-November-00**

Distribution:

XMM-OM Project Office	A Dibbens	Orig.
Mullard Space Science Laboratory	K Mason T Kennedy B Hancock A Smith	
	A Breeveld S Rosen H Kawakami	

Detector System Design II
--- Coincidence for a point source object

24 November 2000
Hajime Kawakami

1. Introduction

Swift UVOT detector employs CCD readout (Fig. 1) coupled with a high sensitivity image intensifier, which pre-amplifies a single photon to 1 million photons before entering the CCD. Because of this high pre-amplification, the CCD can count individual photons. The gain of the intensifier fluctuates event by event randomly, and varies across the field systematically. These unfavourable characteristics can be suppressed down to negligible level by counting photons. There are tiny but many dark events originated in MCP pores. Since these are also discriminated when counting photons, a long integration of image can be done without cooling. Photon splash at phosphor screen of the intensifier has relatively large spatial spread, which causes loss of resolution. By calculating centre of the individual splash (hereafter, "Centroiding") in the photon counting mode, the resolution can be restored or even improved down to sub-CCD pixel level.

The disadvantage of photon counting is small dynamic range. The frame rate of our 10MHz CCD camera is 100 frames/sec with the CCD readout format of 256(H)x256(V). The input count rate of a point source object must be lower than 10 counts/sec to keep coincidence probability lower than 10%. Under this limitation, only <100 photons can be acquired in 10 sec. Therefore, our photon counting detector cannot achieve 10% accuracy for any point source object with 10 sec time resolution.

The centroiding requires 3x3 CCD array for each event. This extendsoverlapping region of the event and jump up coincidence probability for a diffuse object. To keep the coincidence lower than 10%, sky background must be lower than 30,000 counts / sec /(whole area), which is far from the required brightness, 200,000 c/s /(whole area).

Our photon counting detector would not be useful for science if restricted to be used under below 10% coincidence condition. The following sections will describe symptoms associated with a high count rate point source object and will provide practical solutions towards Swift-project.

2. Dynamic range for point source object

The image of 8 pinholes were projected on DEP_#5 intensifier through a fast F-ratio IPCS lens. A thin opaque layer, corresponding to ND2.0 filter, was deposited beneath 3 pinholes (hereafter Spot-1, 2 and 3) to create low intensity pinholes. These 3 pinholes were used for determining brightness of other pinholes during high illumination. The light source consists of 64 green LED array covered with a green narrow band filter (530-570nm) and a diffuser. The distance of the pinholes to the diffuser is 34mm, so that the 8 pinholes were illuminated uniformly by each of the 64 LEDs. The LEDs were driven by a constant current source. The brightness was changed by the current in 5 fixed levels. The characteristics of the individual LEDs to different current may be slightly, but the diffuser keeps the brightness ratio among the 8 pinholes constant. The nominal driving current for the LEDs are 10-20mA, but they were driven in the very low current, 0.02-0.49mA, to produce faint light. Therefore, the stability of the light source might not be excellent. The details of the light source is described in Ref-[1]. This time, a new mask pattern with small pinhole diameter was used. The projected image on the detector was 15um and the acquired image in the photon counting detector was 22um.

Table 1. LED current level

level	1	2	3	4	5
current	0.02	0.05	0.10	0.20	0.49 mA

nominal = 10-20mA

Fig. 2 shows sequence of the measurements for the lowest illumination, i.e. LED level=1. The CCD readout formats were changed from 256(H)x256(V) to 256(H)x16(V) to investigate the improvement of dynamic range with speeding up frame rate. The vertical streaks crossing the bright pinholes are smear due to frame transfer period. They became more significant with the smaller CCD format. The count rate of the bright pinholes was kept below 4 c/s, but it made the faint pinholes was fainter than 0.06 c/s. As the consequence, the integration time had to be 8 hours to give 1000 integrated counts for the faint pinholes. The 3 faint pinholes and the adjacent 3 bright pinholes (hereafter Spot-4, 5 and 6) were used for analysis (see Fig. 3). The CCD camera format was decreased with the measurement sequence in the first half cycle, then increased in the latter half. This can separate the time variation of the light source from the intrinsic variations of the photon counting detector. Figs. 4a,b - 8a,b show detected count rates of the 6 pinholes with the 5 CCD camera formats and in the 5 LED levels without coincidecnce correction either dead time correction. A diaphram of D=407um around a pinhole was used for pinhole photometry. The residual 911x911 um square region was used for background subtraction.

Fig. 4a shows decrease of count rate at CCD format of 256(H)x16(V) and 256(H)x32(V). These are due to photon loss during frame the transfer period. The lower count rate at the 1st measurement (elapsed time = 8 hours) seems to be due to light source, in which the LEDs did not reach steady state yet. Fig. 5a also shows the decrease at CCD format of 256(H)x16(V) and 256(H)x32(V). Slight falls of count rate at 256(V) in the both ends of the measurement are true, since the faint pinholes do not show the fall in Fig. 5b. These are due to photon loss by coincidence. The falls of count rate at larger CCD formats becomes more significant in the higher count rate (i.e. LED level=4) as shown in Fig. 7a. There is no corresponding fall for faint pinholes in Fig. 7b. The lower count rate at CCD format of 16(V) are still noticeable in Figs. 7a. The falls at high count rate are the dominant feature in the very high count rate (i.e. LED level=5) as shown in Fig. 8a. This shows recovery of coincidence loss with the faster frame rate. The effect of the frame transfer period is not apparent.

Table 2 summarizes detected count rates in the 4 LED levels. Table 3 shows relative count rates normalized by the average of 3 faint pinholes. The relative brightness of the 3 individual faint pinholes was determined from the 4 LED levels in order to improve photon statistics and was listed at the bottom of Table 3. The relative brightness of the 3 bright pinholes was determined from LED level = 1 in order to avoid coincidence problem. The coincidence correction was not applied for the 6 values. Inaccuracies due to the photon loss is expected to be less than 2%. The frame transfer period does not affect the ratio of pinhole brightness in these low count rates.

LED level	Exp (sec)	Spot -1	Spot -2	Spot -3	Spot -4	Spot -5	Spot -6	Average -1,2,3
1	28800	.033	.044	.058	3.041	3.977	4.014	.045
2	10800	.125	.193	.234	11.772	15.245	15.377	.184
3	3600	.340	.512	.623	29.415	36.473	36.850	.492
4	1800	.928	1.437	1.735	55.142	62.142	62.762	1.367

Table 2. Detected count rates averaged over all CCD formats. unit:c/s

LED level	Exp (sec)	Spot -1	Spot -2	Spot -3	Spot -4	Spot -5	Spot -6	Average of -1,2,3
1	28800	.683	1.042	1.275	67.742	88.613	89.471	1.000
2	10800	.692	1.041	1.268	67.376	87.995	88.903	1.000
3	3600	.681	1.042	1.277	65.024	83.617	84.212	1.000
4	1800	.679	1.044	1.277	55.039	67.805	67.785	1.000
***		.684	1.042	1.274	67.742	88.613	89.471	1.000

Table 3. Relative detected count rates to 3 faint pinholes

Fig. 9 shows the detected count rate against input count rate in various CCD formats. Where, the input count rates for the 3 bright pinholes were estimated from the average of 3 faint pinholes. Again, neither dead time correction nor coincidence correction was applied for both of abscissa and ordinate in this diagram. Fig. 10 is the magnified diagram at the higher count rate end. Deviation from the linear relation occurs at the lower count rate with the larger CCD format, i.e. the slower frame rate. These figures are expressed in Log-Log scale, therefore the true damage of data quality is modestly shown. Fig. 11 shows the ratio of detected count rate to input rate. The ordinate is in linear scale. The saturation effect is obvious at the count rate of 10% of the frame rate. The dynamic range is expanded in the smaller CCD format.

3. Count rate correction for point source object

Our intensifier employs fast phosphor screen, P46, whose decay time is 300ns from 90% to 10% and 90us from 10% to 1%. Any event does not persist until next frame in our CCD readout, which is separated by frame transfer period of 174us. Therefore, the event is not counted twice in the different 2 frames. Events from a point source overlapp on top of others in good optics. Therefore, multiple events are counted as only "1", even if many arrive in a single CCD frame.

In these simple conditions, there is an exact solution to equate event detection probability (or event loss probability) as described below (Ref. Kawakami and Fordham 1998 [1]),

$$p = \frac{1 - \exp(-x/FR)}{x/FR} ,$$

$$x = c * FR * (1/FR - FT) \qquad \text{(Eq. 1).}$$

Where, p denotes detection probability, c incoming event rate, FR frame rate, FT frame transfer period. Eq. 1 is converted to the following for the convenience of estimation of the incoming event rate,

$$c = -\ln\left(1 - \frac{c\_det}{FR}\right) / (1/FR - FT) \qquad \text{(Eq. 2).}$$

Where, c_det denotes detected count rate in the photon counting image.

Table 4. Frame period and dead time ratio of CCD camera

V_length	FR_period	Dead time ratio	FT period
256	1.087260E-02	2.119088E-02	2.304000E-04
128	5.727000E-03	4.023049E-02	2.304000E-04
64	3.154200E-03	7.304546E-02	2.304000E-04
32	1.867800E-03	1.233537E-01	2.304000E-04
16	1.224600E-03	1.881431E-01	2.304000E-04

unit: second

All data, even for the faint pinholes, were converted to the true incoming rate using Eq. 2. Frame period of CCD camera and Frame Transfer period for this calculation are tabulated in Table 4. The revised response curve is shown in Fig. 12. Where, tiny coincidence correction were applied for the 3 faint pinholes to calculate the abscissa, input count rate. The dead time correction due to frame transfer period was also applied. The ordinate was replaced by count rate corrected for coincidence and dead time. The linearity range looks to be expanded dramatically in this Log-Log scale description, but over corrections at high count rate are noticeable. Figs. 13 and 14 show the ratio of corrected count rate to input count rate in linear scale with the larger CCD format and the smaller CCD format. The corrections were useful if the count rate was lower than 20% of frame rate. But, was not useful or even harmful for the count rate higher than 100% of frame rate.

4. Dead time correction

Our photon counting detector does not allocate photons at the pinhole position in its frame memory during frame transfer period. Therefore, photons are effectively lost if a diaphram for photometry is sensively small. For example, Fig 5a shows falls of detected count rate at small CCD formats, 256(H)x16(V) and 256(H)x32(V). It is possible to estimate this dead time accurately with the fast P-46 phosphor screen, and then restore absolute brightness. This correction is already included in Eq. 2 in the previous section. Fig. 15 shows the diagram after the correction. The count rate becomes flat along various CCD format sizes. This is a strong evidence for the validity of the dead time correction. Fig. 16 is other example of the dead time correction corresponding to Fig. 6a, in the higher count rate. The slight concave shape is due to inaccuracies of coincidence correction. Fig. 17a is even in higher count rate. The convex shape is due to the coincidence correction error. The same measurement for the faint pinholes deos not show the concave shape (see Fig. 17b). Therefore, it is not due to the light source variation.

5. Challenge to extremely high count rate

The coincidence correction for a point source object should be very accurate if the image is really sharp. But, there are small aberration, diffraction pattern and scattered light in the real optics. The photon counting detector itself contains image blurring due to photocathode gap and centroiding error. These causes faint wing component around core image. The wind component starts playing significant role in coincidence loss for a very bright star. The diameter of diaph was D=407um , i.e. 5.25 CCD pixel in previous sections. This picked up almost all photons around a pinhole. This is, however, conflict with the assumption of point source. If two photons arrived in the spatial separation of 2 CCD pixels, both of the two photons could be detected by the system. So, the number of detected eventseasily exceeds total frame number for high count rate pinholes.

Table 5. Extent of detected events around pinholes (LED level=4)

CCD Format	Pinhole	Sampling Region (CCD pixel) 1x1	2x2	3x3	4x4	5x5
256V	1	.78717	.89506	.98581	.99557	1.00000
256V	2	.70393	.96812	.98375	.99618	1.00000
256V	3	.45366	.95321	.96260	.98485	1.00000
256V	4	.65470	.94674	.96638	.98441	1.00000
256V	5	.59537	.94551	.96108	.97874	1.00000

256V	6	.59489	.94481	.96271	.97820	1.00000
16V	1	.82897	.92724	.98467	.99551	1.00000
16V	2	.76166	.97428	.98437	.99964	1.00000
16V	3	.47402	.95669	.96577	.98579	1.00000
16V	4	.58500	.94611	.96893	.98770	1.00000
16V	5	.53202	.94517	.96600	.98657	1.00000
16V	6	.58449	.94409	.96801	.98579	1.00000

Pinhole 1-3: 1 - 2 c/s
Pinhole 4-6: 60-100 c/s

Table 5 shows point spread function of pinhole images. Since count rate is lower than 2.0 c/s for the 3 faint pinholes (i.e. 1-3), the table shows almost true photon distribution. The bright 3 pinholes (i.e. 4-5) contain some saturation effect due to coincidence. It would be perfect if all photons fall into one CCD pixel to apply Eq.2. This, however, never happends because the pinhole image can be located at the boundary of 2 CCD pixels. The equation is still mathematically correct if all photons fall into 2x2 CCD array, since our digital processor captures only "one" event within any consecutive 2 CCD pixels. The table shows 90% of photons fall into the 2x2 CCD array. The worst location of pinhole image is at the centre of CCD pixel for the 2x2 CCD sample (see Spot-1). Since event splash at phosphor screen has spatial extent of ~1.0 CCD pixel(FWHM), 2 events in the separation of 2 CCD pixels can be merged together in a CCD image. In such case, Eq 2 is again valid for 3x3 CCD array sampling. The table shows more than 96% of photons fall into the 3x3 CCD array. The best location of pinhole for the 3x3 sampling is at the centre of CCD pixel.

For simplicities, we assume 2 cases;
1) all photons fall into 2x2 CCD array with 100% coincidence among the photons,
2) all photons fall into 3x3 CCD array with 100% coincidence among the photons.

Fig. 18 shows the count rates of the bright pinholes in the LED level=5 at various CCD formats after the standard correction, i.e. sampled with the diaphram of D=5.25 CCD pixel. It starts showing over correction from the CCD format 256(H)x64(V) for Spot-4, i.e. frame rate of 317 FRs/s against event rate of 500c/s. The correction became infinity at CCD format 256(H)x128(V) for Spots-5 and-6, i.e. frame rate of 175 FRs/s against event rate of 600c/s. Fig. 19a is with the 3x3 CCD array sampling. The dynamic rage looks more expanded. Fig. 19b is with the 2x2 CCD array sampling. The corrected count rates looks flat up to 256(H) x128(V) for Spot-4, though showing over correction for Spots-5 and -6.

Figs. 20a and 20b show accuracies of the corrections with the 3x3 CCD array and the 2x2 CCD array saplings at large CCD formats, corresponding to Fig. 13 with standard sampling. The input count rates in these new figures werer hired from Fig. 13. The corrected count rates were consistently lower than 1.0 with the 2x2 CCD array sampling as agreed with Table 5. This can be usable up to 600 c/s with CCD format 256(H)x128(V), at the expense of under estimation by 20%max. It is recommended that pinhole image should be sampled by 2x2 CCD array when input count rate is higher than 1.0 time of frame rate but lower than 3.4 times. The standard sampling is more accurate for the lower count rate.

The detected count rate per frame becomes very close to 1.0 at this extreme high count rate regime. Tiny fraction from the 1.0 determine the true input rate. Therefore, extreme high precision measurements are required. For instance, if exposure time or frame rate of CCD camera were mis-calculated in a few %, it easily cost a few 10% in the corrected count rate.

This experiment was carried out with the XMM-OM's BPU ver "engineering phase-1". This original BPU contains design problem, which can count one event as "2" when the event strikes at the corner of a CCD pixel. This problem was completely fixed at XMM-OM's QM-phase as a major design change. The detected count rate must not exceed frame rate when sampled by 2x2 CCD array as explained above. But, it actually happened in this experiment at CCD format 256(H)x256(V) for Spots -5 and -6. The validity of the 2x2 CCD array sample at very high count rate (e.g. > 3 times of frame rate) must be tested with the improved BPUs.

Ref.
[1] H. Kawakami, "Intense illumination of DEP_#8 intensifier", XMM-OM/MSSL/TC/0057 (1999)
[2] H. Kawakami and J. Fordham, "Flat Field coincidence loss in the MIC detector for XMM-OM", XMM-OM/MSSL/TC/0050 (1998)

Appendix. Measurements used for this report

```
----------------------------------------------------------------------------------------------------
Cal160 Sgl L=3    1000S   CCDST=(65,17)256V  (1200,1144)    IPCS  DEP_#5
     13H 42M 12S       13H 58M 52S       2000/11/03
Cal161 Sgl L=3    1000S   CCDST=(65,81)128V  (1200,0632)    IPCS  DEP_#5
     13H 59M 17S       14H 15M 57S       2000/11/03
Cal162 Sgl L=3    1000S   CCDST=(65,113)64V  (1200,0400)    IPCS  DEP_#5
     14H 16M 22S       14H 33M 02S       2000/11/03
Cal163 Sgl L=3    1000S   CCDST=(65,129)32V  (1200,0400)    IPCS  DEP_#5
     14H 33M 27S       14H 50M 07S       2000/11/03
Cal164 Sgl L=3    1000S   CCDST=(65,137)16V  (1200,0400)    IPCS  DEP_#5
     14H 50M 32S       15H 07M 12S       2000/11/03
Cal165 Sgl L=3    1000S   CCDST=(65,137)16V  (1200,0400)    IPCS  DEP_#5
     15H 07M 38S       15H 24M 18S       2000/11/03
Cal166 Sgl L=3    1000S   CCDST=(65,129)32V  (1200,0400)    IPCS  DEP_#5
     15H 24M 43S       15H 41M 23S       2000/11/03
Cal167 Sgl L=3    1000S   CCDST=(65,113)64V  (1200,0400)    IPCS  DEP_#5
     15H 41M 48S       15H 58M 28S       2000/11/03
Cal168 Sgl L=3    1000S   CCDST=(65,81)128V  (1200,0632)    IPCS  DEP_#5
     15H 58M 53S       16H 15M 33S       2000/11/03
Cal169 Sgl L=3    1000S   CCDST=(65,17)256V  (1200,1144)    IPCS  DEP_#5
     16H 15M 58S       16H 32M 38S       2000/11/03
Cal170 Sgl L=4    0600S   CCDST=(65,17)256V  (1200,1144)    IPCS  DEP_#5
     16H 38M 21S       16H 48M 21S       2000/11/03
Cal171 Sgl L=4    0600S   CCDST=(65,81)128V  (1200,0632)    IPCS  DEP_#5
     16H 48M 46S       16H 58M 46S       2000/11/03
Cal172 Sgl L=4    0600S   CCDST=(65,113)64V  (1200,0400)    IPCS  DEP_#5
     16H 59M 11S       17H 09M 11S       2000/11/03
Cal173 Sgl L=4    0600S   CCDST=(65,129)32V  (1200,0400)    IPCS  DEP_#5
     17H 09M 36S       17H 19M 36S       2000/11/03
```

```
Cal174 Sgl L=4   0600S   CCDST=(65,137)16V  (1200,0400)   IPCS  DEP_#5
     17H 20M 01S      17H 30M 01S      2000/11/03
Cal175 Sgl L=4   0600S   CCDST=(65,137)16V  (1200,0400)   IPCS  DEP_#5
     17H 30M 26S      17H 40M 26S      2000/11/03
Cal176 Sgl L=4   0600S   CCDST=(65,129)32V  (1200,0400)   IPCS  DEP_#5
     17H 40M 51S      17H 50M 51S      2000/11/03
Cal177 Sgl L=4   0600S   CCDST=(65,113)64V  (1200,0400)   IPCS  DEP_#5
     17H 51M 16S      18H 01M 16S      2000/11/03
Cal178 Sgl L=4   0600S   CCDST=(65,81)128V  (1200,0632)   IPCS  DEP_#5
     18H 01M 41S      18H 11M 41S      2000/11/03
Cal179 Sgl L=4   0600S   CCDST=(65,17)256V  (1200,1144)   IPCS  DEP_#5
     18H 12M 06S      18H 22M 06S      2000/11/03
Cal180 Sgl L=5   0300S   CCDST=(65,17)256V  (1200,1144)   IPCS  DEP_#5
     18H 31M 11S      18H 36M 11S      2000/11/03
Cal181 Sgl L=5   0300S   CCDST=(65,81)128V  (1200,0632)   IPCS  DEP_#5
     18H 36M 36S      18H 41M 36S      2000/11/03
Cal182 Sgl L=5   0300S   CCDST=(65,113)64V  (1200,0400)   IPCS  DEP_#5
     18H 42M 01S      18H 47M 01S      2000/11/03
Cal183 Sgl L=5   0300S   CCDST=(65,129)32V  (1200,0400)   IPCS  DEP_#5
     18H 47M 26S      18H 52M 26S      2000/11/03
Cal184 Sgl L=5   0300S   CCDST=(65,139)16V  (1200,0400)   IPCS  DEP_#5
     18H 52M 51S      18H 57M 51S      2000/11/03
Cal185 Sgl L=5   0300S   CCDST=(65,139)16V  (1200,0400)   IPCS  DEP_#5
     18H 58M 16S      19H 03M 16S      2000/11/03
Cal186 Sgl L=5   0300S   CCDST=(65,129)32V  (1200,0400)   IPCS  DEP_#5
     19H 03M 41S      19H 08M 41S      2000/11/03
Cal187 Sgl L=5   0300S   CCDST=(65,113)64V  (1200,0400)   IPCS  DEP_#5
     19H 09M 06S      19H 14M 06S      2000/11/03
Cal188 Sgl L=5   0300S   CCDST=(65,81)128V  (1200,0632)   IPCS  DEP_#5
     19H 14M 31S      19H 19M 31S      2000/11/03
Cal189 Sgl L=5   0300S   CCDST=(65,17)256V  (1200,1144)   IPCS  DEP_#5
     19H 19M 56S      19H 24M 56S      2000/11/03
Cal190 Sgl L=1  28800S   CCDST=(65,17)256V  (1200,1144)   IPCS  DEP_#5
     19H 43M 05S      03H 43M 05S      2000/11/03
Cal191 Sgl L=1  28800S   CCDST=(65,81)128V  (1200,0632)   IPCS  DEP_#5
     03H 43M 30S      11H 43M 30S      2000/11/04
Cal192 Sgl L=1  28800S   CCDST=(65,113)64V  (1200,0400)   IPCS  DEP_#5
     11H 43M 55S      19H 43M 55S      2000/11/04
Cal193 Sgl L=1  28800S   CCDST=(65,129)32V  (1200,0400)   IPCS  DEP_#5
     19H 44M 20S      03H 44M 20S      2000/11/04
Cal194 Sgl L=1  28800S   CCDST=(65,139)16V  (1200,0400)   IPCS  DEP_#5
     03H 44M 45S      11H 44M 45S      2000/11/05
Cal195 Sgl L=1  28800S   CCDST=(65,139)16V  (1200,0400)   IPCS  DEP_#5
     11H 45M 10S      19H 45M 10S      2000/11/05
Cal196 Sgl L=1  28800S   CCDST=(65,129)32V  (1200,0400)   IPCS  DEP_#5
     19H 45M 35S      03H 45M 35S      2000/11/05
Cal197 Sgl L=1  28800S   CCDST=(65,113)64V  (1200,0400)   IPCS  DEP_#5
     03H 46M 00S      11H 46M 00S      2000/11/06
Cal198 Sgl L=1  28800S   CCDST=(65,81)128V  (1200,0632)   IPCS  DEP_#5
     11H 46M 25S      19H 46M 25S      2000/11/06
Cal199 Sgl L=1  28800S   CCDST=(65,17)256V  (1200,1144)   IPCS  DEP_#5
     19H 46M 50S      03H 46M 50S      2000/11/06
Cal200 Sgl L=2  10800S   CCDST=(65,17)256V  (1200,1144)   IPCS  DEP_#5
     10H 35M 21S      13H 35M 21S      2000/11/07
Cal201 Sgl L=2  10800S   CCDST=(65,81)128V  (1200,0632)   IPCS  DEP_#5
     13H 35M 46S      16H 35M 46S      2000/11/07
Cal202 Sgl L=2  10800S   CCDST=(65,113)64V  (1200,0400)   IPCS  DEP_#5
     16H 36M 22S      19H 36M 22S      2000/11/07
Cal203 Sgl L=2  10800S   CCDST=(65,129)32V  (1200,0400)   IPCS  DEP_#5
     19H 36M 47S      22H 36M 47S      2000/11/07
Cal204 Sgl L=2  10800S   CCDST=(65,139)16V  (1200,0400)   IPCS  DEP_#5
     22H 37M 12S      01H 37M 12S      2000/11/07
Cal205 Sgl L=2  10800S   CCDST=(65,139)16V  (1200,0400)   IPCS  DEP_#5
     01H 37M 37S      04H 37M 37S      2000/11/08
Cal206 Sgl L=2  10800S   CCDST=(65,129)32V  (1200,0400)   IPCS  DEP_#5
     04H 38M 02S      07H 38M 02S      2000/11/08
```

```
Cal207 Sgl L=2  10800S  CCDST=(65,113)64V  (1200,0400)   IPCS  DEP_#5
     07H 38M 27S     10H 38M 27S     2000/11/08
Cal208 Sgl L=2  10800S  CCDST=(65,81)128V  (1200,0632)   IPCS  DEP_#5
     10H 38M 52S     13H 38M 52S     2000/11/08
Cal209 Sgl L=2  10800S  CCDST=(65,17)256V  (1200,1144)   IPCS  DEP_#5
     13H 39M 17S     16H 39M 17S     2000/11/08
Cal210 Sgl L=3   3600S  CCDST=(65,17)256V  (1200,1144)   IPCS  DEP_#5
     10H 42M 31S     11H 42M 31S     2000/11/09
Cal211 Sgl L=3   3600S  CCDST=(65,81)128V  (1200,0632)   IPCS  DEP_#5
     11H 43M 13S     12H 43M 13S     2000/11/09
Cal212 Sgl L=3   3600S  CCDST=(65,113)64V  (1200,0400)   IPCS  DEP_#5
     12H 43M 38S     13H 43M 38S     2000/11/09
Cal213 Sgl L=3   3600S  CCDST=(65,129)32V  (1200,0400)   IPCS  DEP_#5
     13H 44M 03S     14H 44M 03S     2000/11/09
Cal214 Sgl L=3   3600S  CCDST=(65,137)16V  (1200,0400)   IPCS  DEP_#5
     14H 44M 28S     15H 44M 28S     2000/11/09
Cal215 Sgl L=3   3600S  CCDST=(65,137)16V  (1200,0400)   IPCS  DEP_#5
     15H 44M 53S     16H 44M 53S     2000/11/09
Cal216 Sgl L=3   3600S  CCDST=(65,129)32V  (1200,0400)   IPCS  DEP_#5
     16H 45M 18S     17H 45M 18S     2000/11/09
Cal217 Sgl L=3   3600S  CCDST=(65,113)64V  (1200,0400)   IPCS  DEP_#5
     17H 45M 43S     18H 45M 43S     2000/11/09
Cal218 Sgl L=3   3600S  CCDST=(65,81)128V  (1200,0632)   IPCS  DEP_#5
     18H 52M 03S     19H 52M 03S     2000/11/09
Cal219 Sgl L=3   3600S  CCDST=(65,17)256V  (1200,1144)   IPCS  DEP_#5
     19H 52M 28S     20H 52M 28S     2000/11/09
Cal220 Sgl L=4   1500S  CCDST=(65,17)256V  (1200,1144)   IPCS  DEP_#5
     10H 38M 47S     11H 03M 47S     2000/11/10
Cal221 Sgl L=4   1500S  CCDST=(65,81)128V  (1200,0632)   IPCS  DEP_#5
     11H 04M 12S     11H 29M 12S     2000/11/10
Cal222 Sgl L=4   1500S  CCDST=(65,113)64V  (1200,0400)   IPCS  DEP_#5
     11H 29M 37S     11H 54M 37S     2000/11/10
Cal223 Sgl L=4   1500S  CCDST=(65,129)32V  (1200,0400)   IPCS  DEP_#5
     11H 55M 02S     12H 20M 02S     2000/11/10
Cal224 Sgl L=4   1500S  CCDST=(65,137)16V  (1200,0400)   IPCS  DEP_#5
     12H 20M 27S     12H 45M 27S     2000/11/10
Cal225 Sgl L=4   1500S  CCDST=(65,137)16V  (1200,0400)   IPCS  DEP_#5
     12H 45M 52S     13H 10M 52S     2000/11/10
Cal226 Sgl L=4   1500S  CCDST=(65,129)32V  (1200,0400)   IPCS  DEP_#5
     13H 11M 17S     13H 36M 17S     2000/11/10
Cal227 Sgl L=4   1500S  CCDST=(65,113)64V  (1200,0400)   IPCS  DEP_#5
     13H 36M 42S     14H 01M 42S     2000/11/10
Cal228 Sgl L=4   1500S  CCDST=(65,81)128V  (1200,0632)   IPCS  DEP_#5
     14H 02M 07S     14H 27M 07S     2000/11/10
Cal229 Sgl L=4   1500S  CCDST=(65,17)256V  (1200,1144)   IPCS  DEP_#5
     14H 27M 32S     14H 52M 32S     2000/11/10
-----------------------------------------------------------------------------------------------------------
```

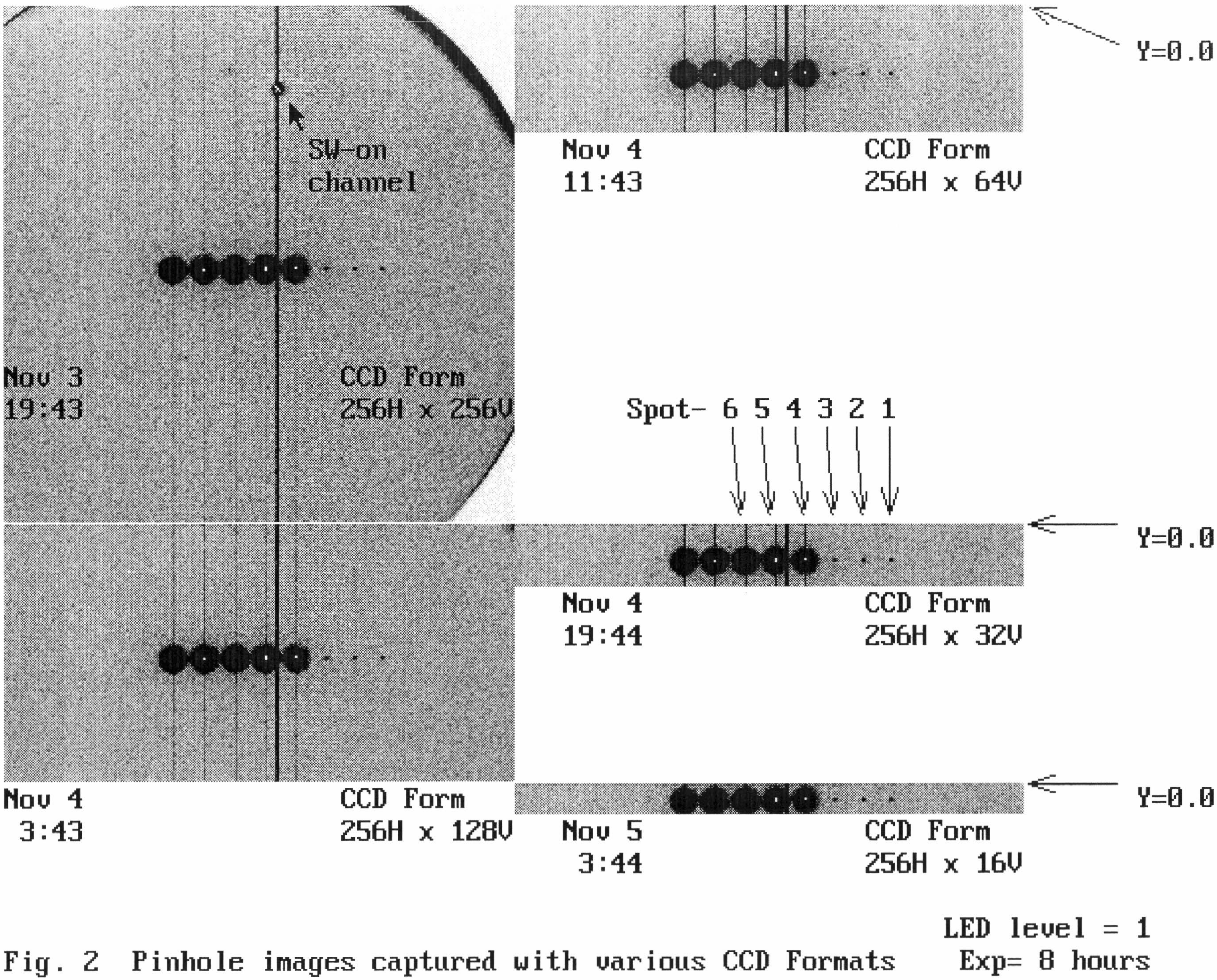

Fig. 2 Pinhole images captured with various CCD Formats

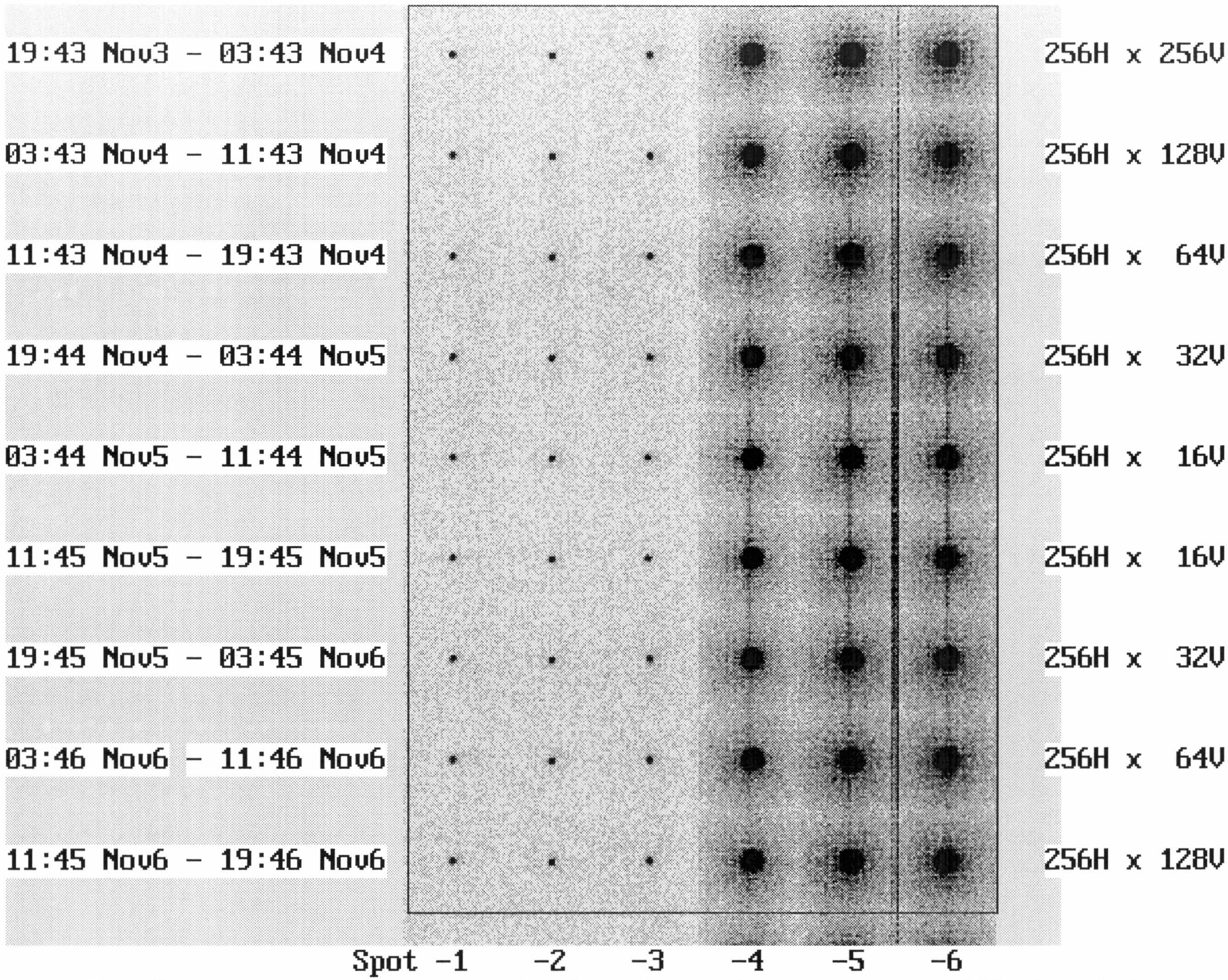

Fig. 3 Sequence of measurements for individual spot LED level=1

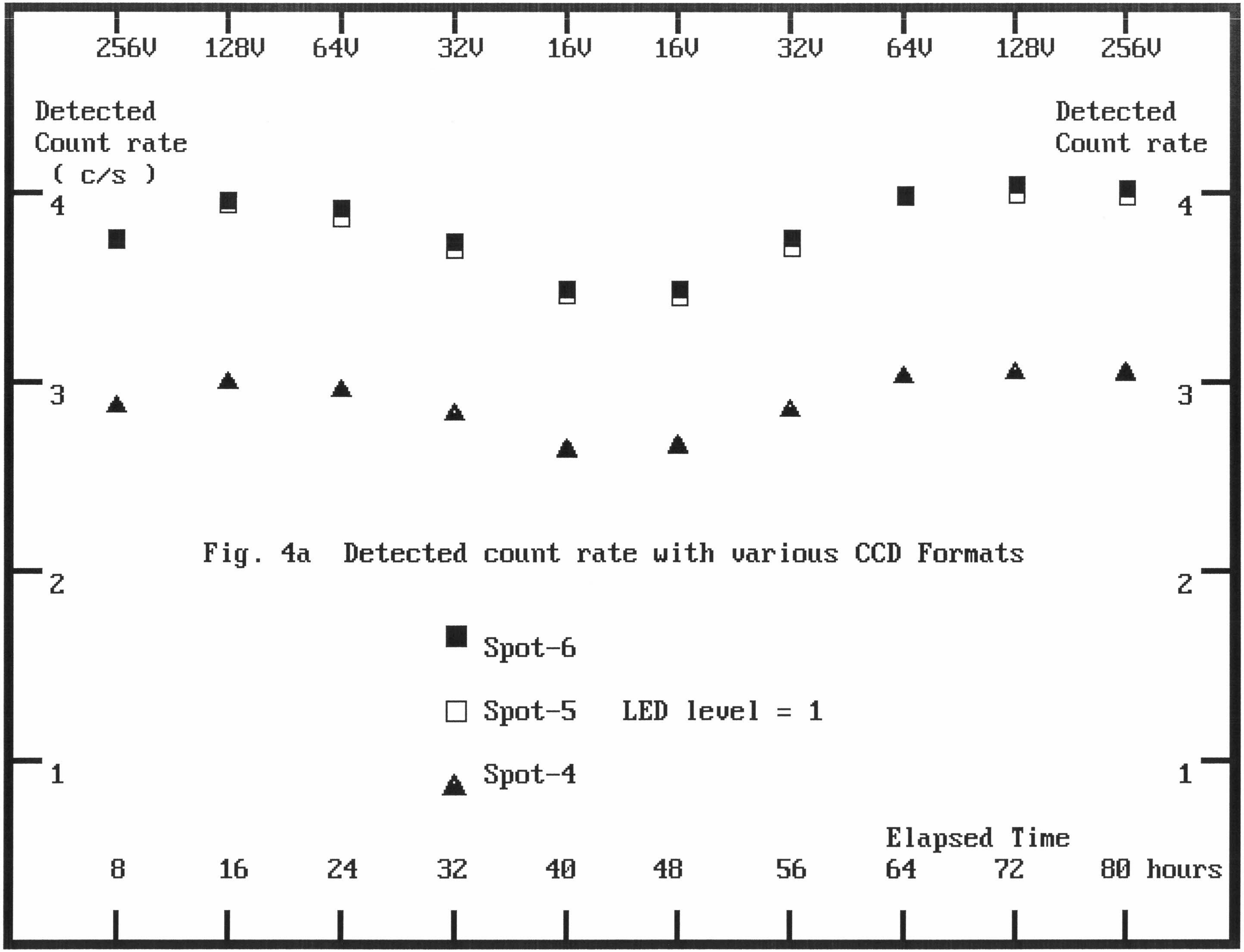

Fig. 4a Detected count rate with various CCD Formats

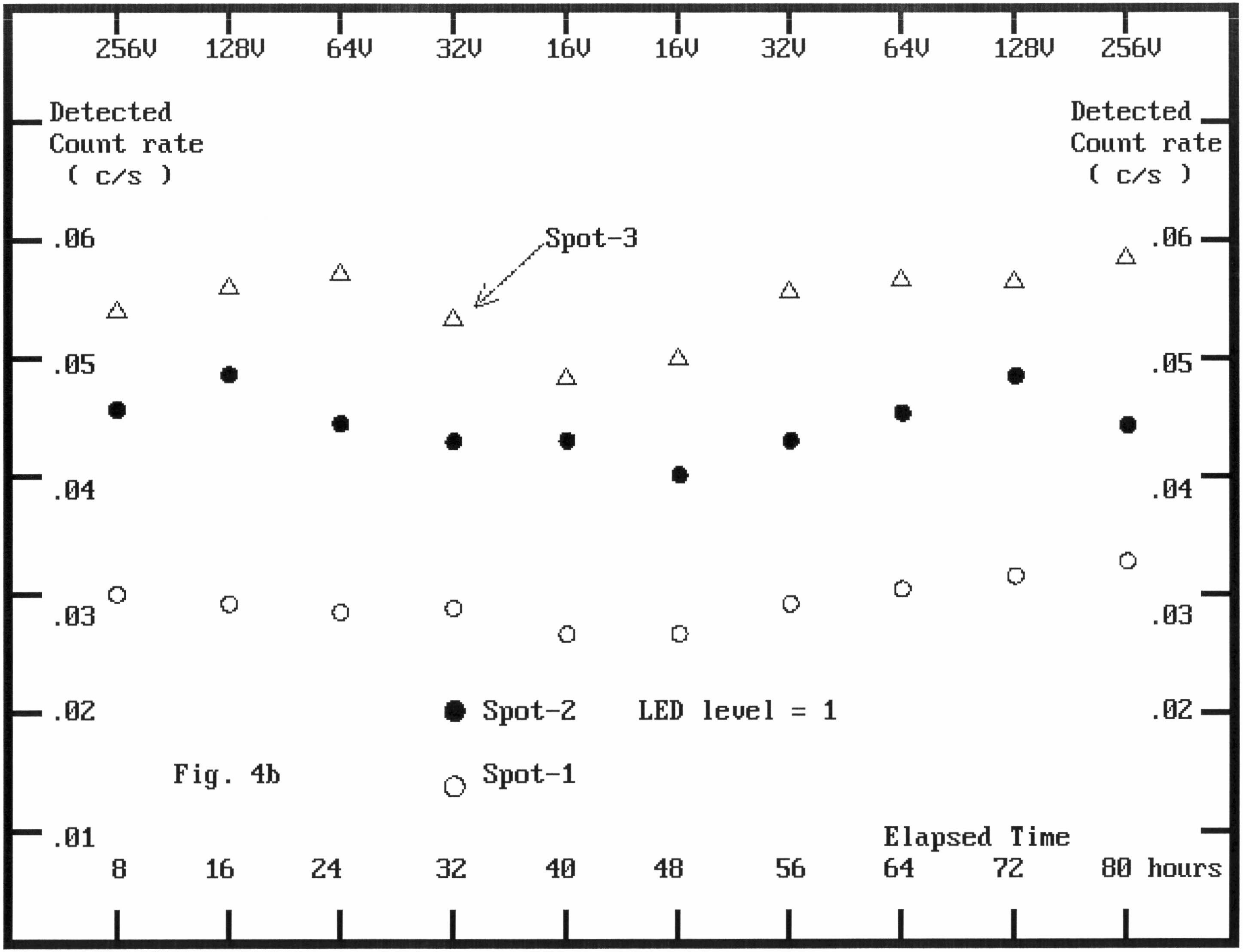
256V
128V
64V
32V
16V
16V
32V
64V
128V
256V
Detected Count rate (c/s)
Detected Count rate (c/s)
.06
.05
.04
.03
.02
.01
Spot-3
Spot-2
LED level = 1
Spot-1
Elapsed Time
8
16
24
32
40
48
56
64
72
80 hours
Fig. 4b

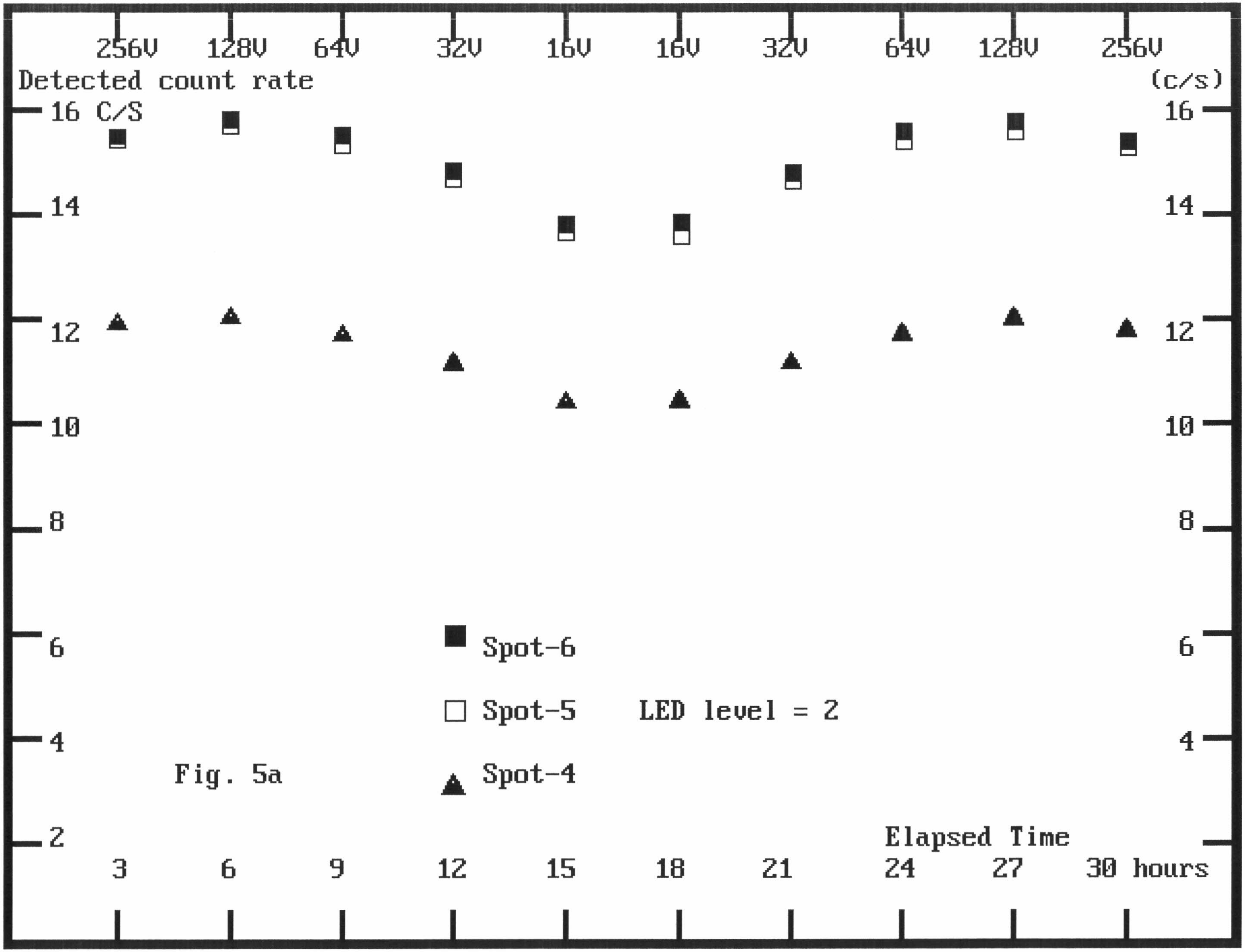

256V
128V
64V
32V
16V
16V
32V
64V
128V
256V
Detected count rate
(c/s)
16 C/S
14
12
10
8
6
4
2
16
14
12
10
8
6
4
Spot-6
Spot-5
LED level = 2
Spot-4
Fig. 5a
Elapsed Time
3
6
9
12
15
18
21
24
27
30 hours

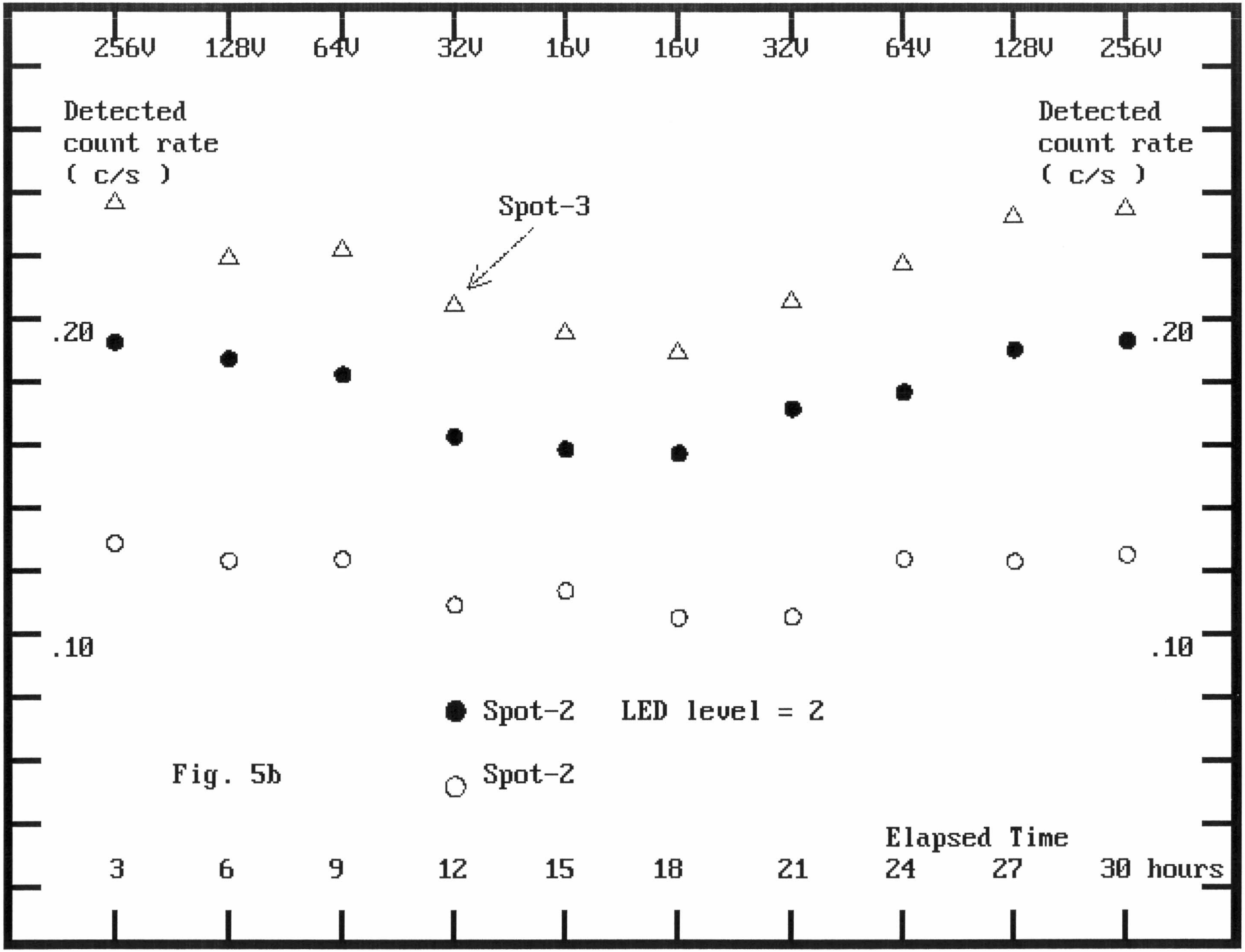
256V
128V
64V
32V
16V
16V
32V
64V
128V
256V
Detected count rate (c/s)
Detected count rate (c/s)
Spot-3
.20
.20
.10
.10
Spot-2 LED level = 2
Fig. 5b
Spot-2
Elapsed Time
3
6
9
12
15
18
21
24
27
30 hours

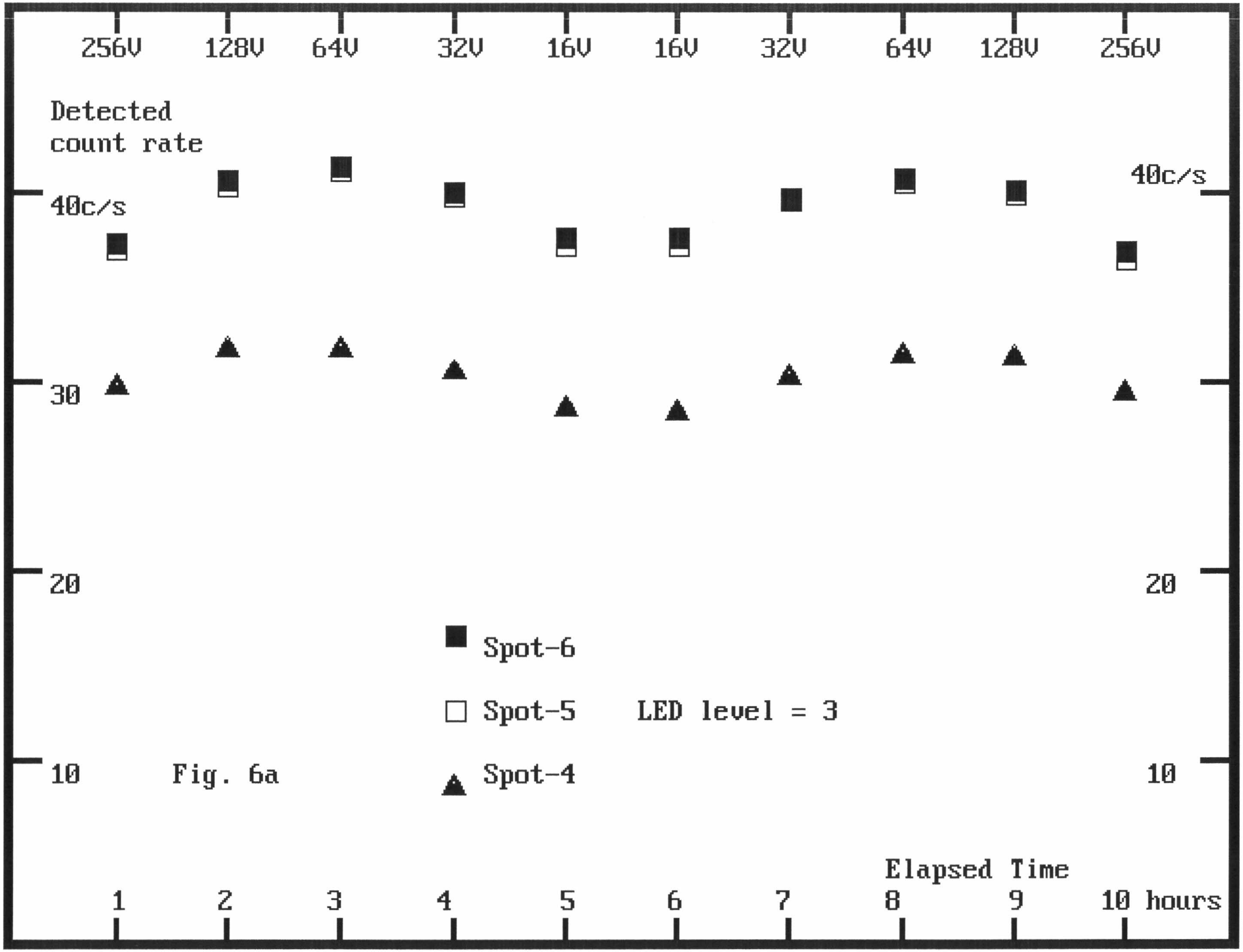
256V
128V
64V
32V
16V
16V
32V
64V
128V
256V
Detected
count rate
40c/s
30
20
10
40c/s
20
10
Spot-6
Spot-5
LED level = 3
Spot-4
Elapsed Time
1
2
3
4
5
6
7
8
9
10 hours
Fig. 6a

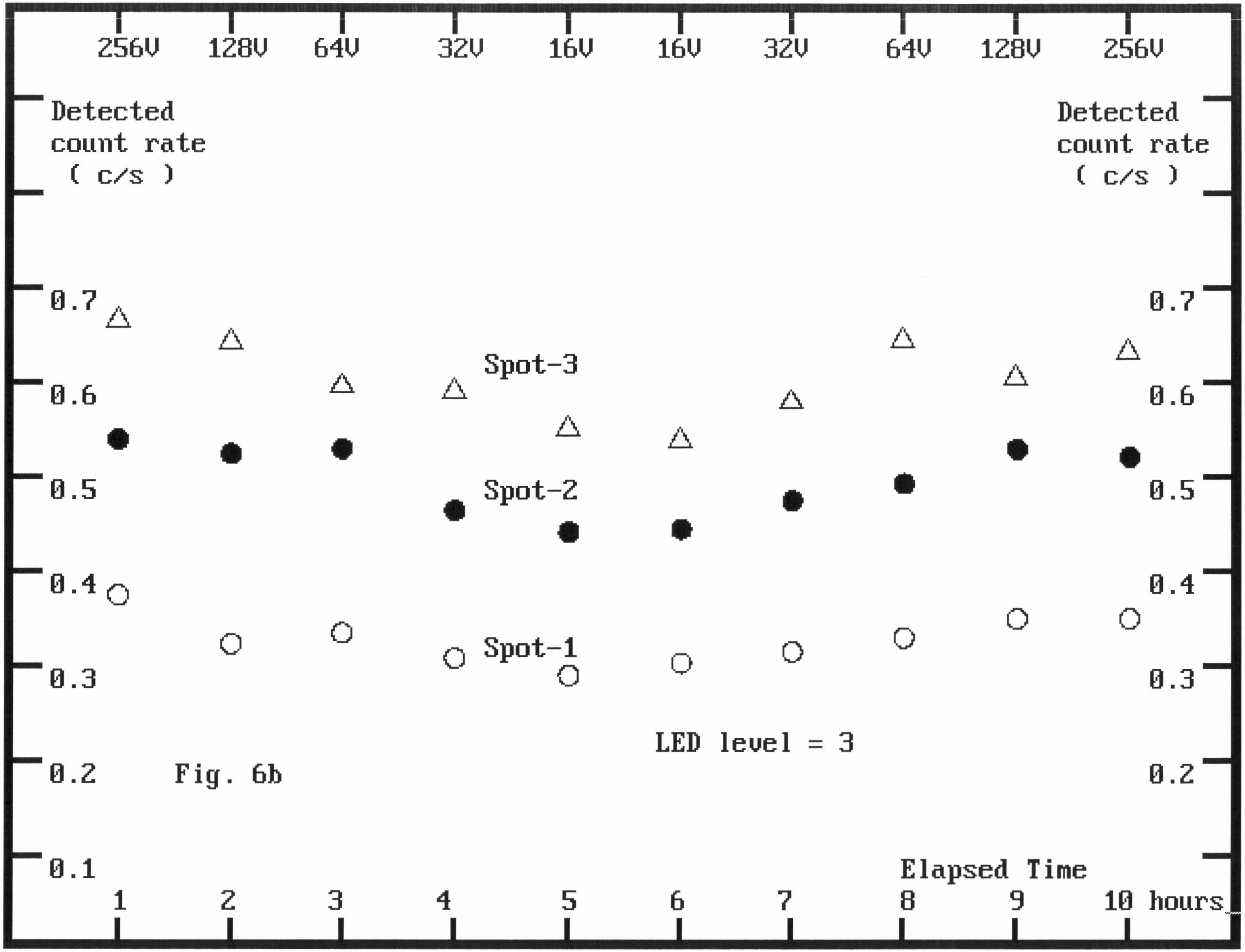
256V 128V 64V 32V 16V 16V 32V 64V 128V 256V
Detected count rate (c/s)
Detected count rate (c/s)
0.7
0.6
0.5
0.4
0.3
0.2
0.1
Spot-3
Spot-2
Spot-1
LED level = 3
Elapsed Time
1 2 3 4 5 6 7 8 9 10 hours
Fig. 6b

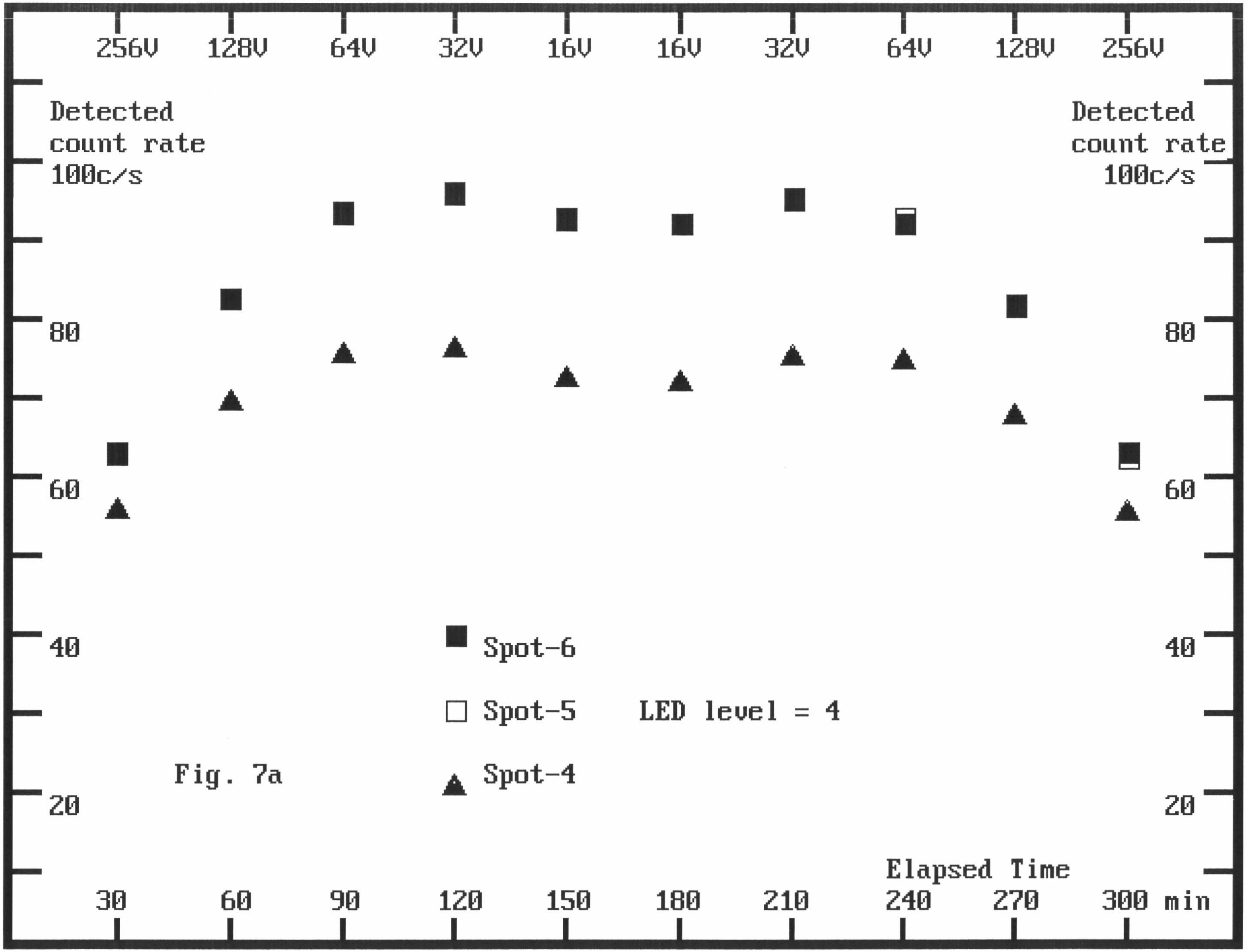
256V 128V 64V 32V 16V 16V 32V 64V 128V 256V
Detected
count rate
100c/s
Detected
count rate
100c/s
80
60
40
20
80
60
40
20
Spot-6
Spot-5
LED level = 4
Spot-4
Elapsed Time
30 60 90 120 150 180 210 240 270 300 min

Fig. 7a

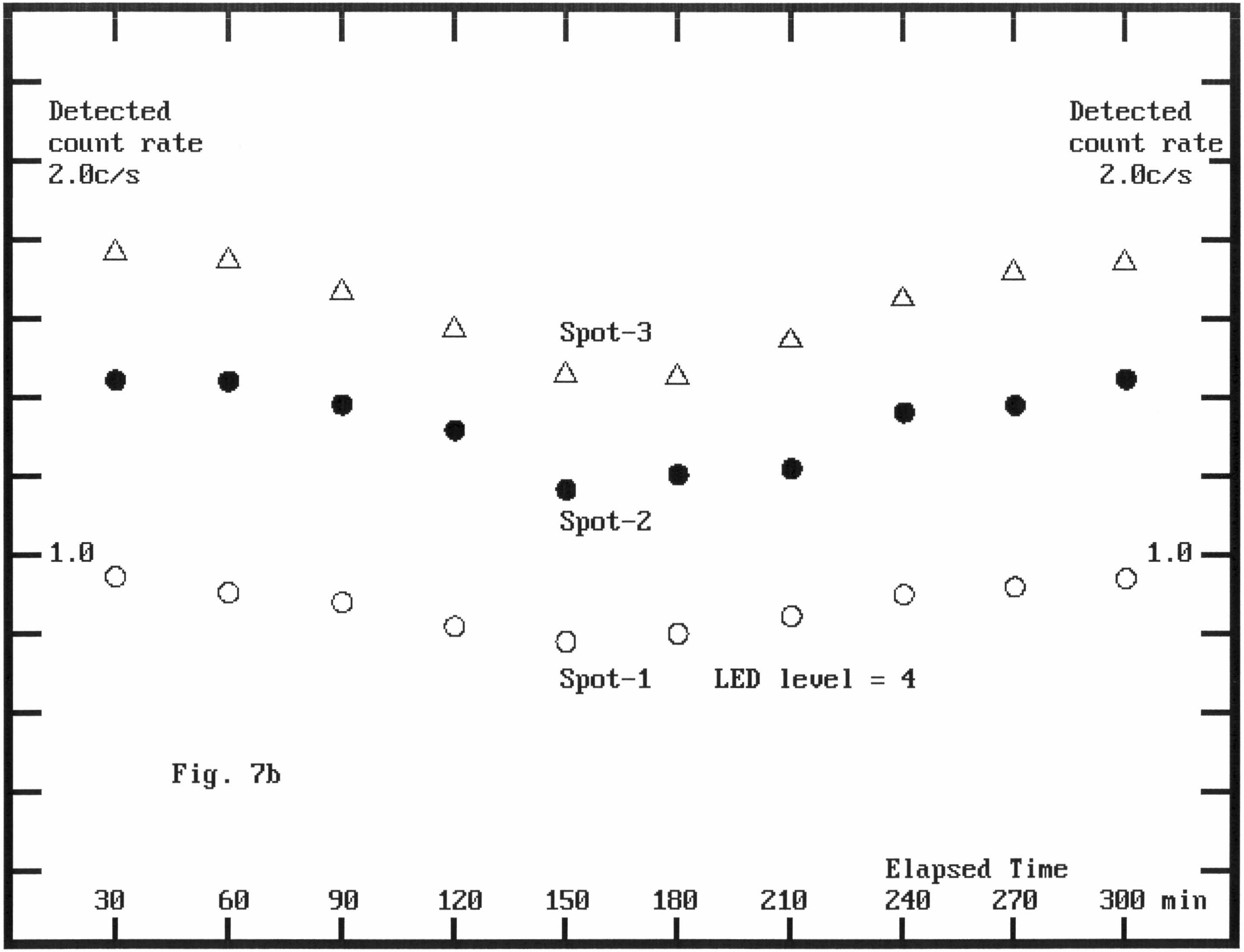
Detected
count rate
2.0c/s
Detected
count rate
2.0c/s
Spot-3
Spot-2
1.0
1.0
Spot-1
LED level = 4
Fig. 7b
Elapsed Time
30
60
90
120
150
180
210
240
270
300 min

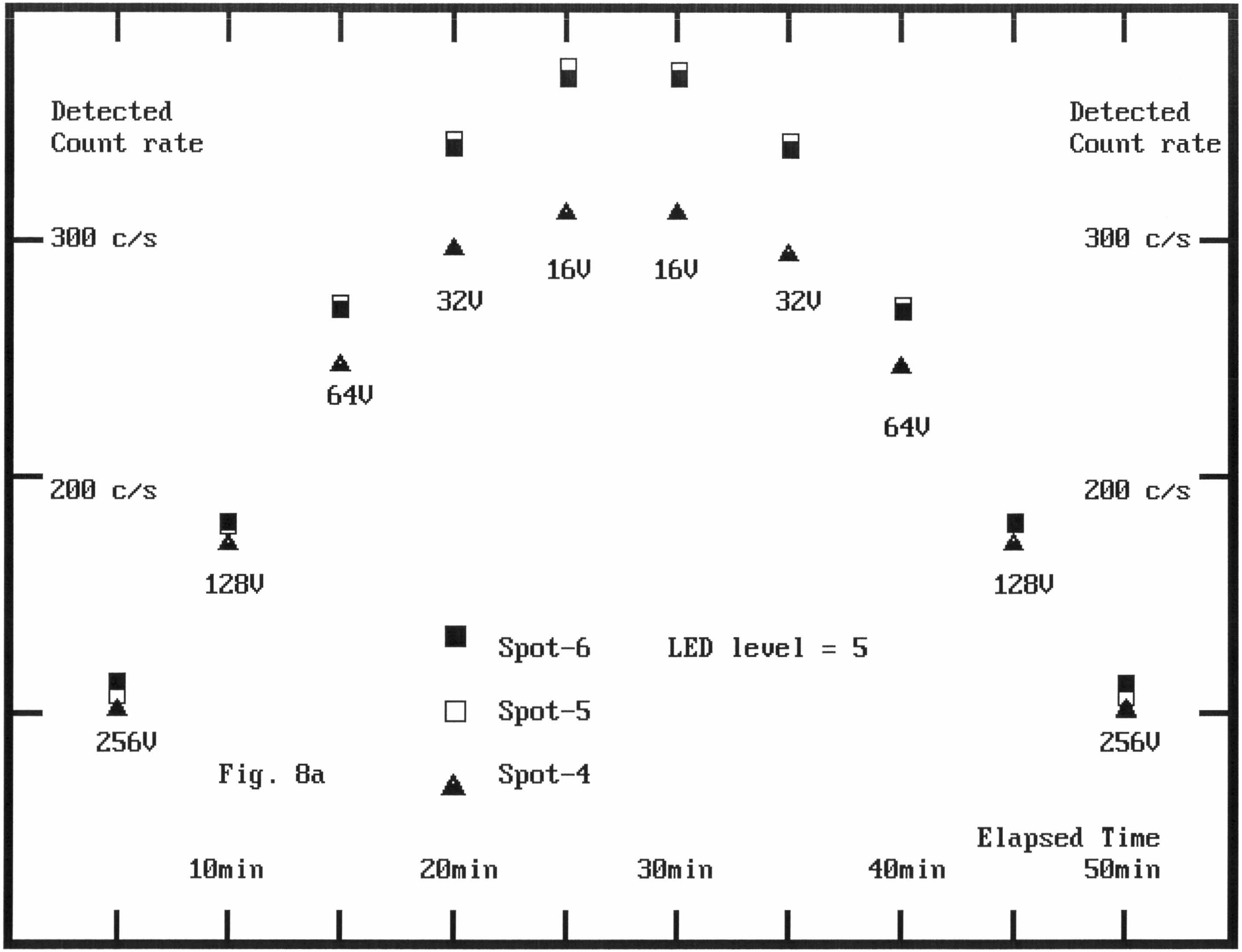

Detected
Count rate
Detected
Count rate
300 c/s
300 c/s
200 c/s
200 c/s
16V
16V
32V
32V
64V
64V
128V
128V
256V
256V
Spot-6
LED level = 5
Spot-5
Spot-4
Elapsed Time
10min
20min
30min
40min
50min

Fig. 8a

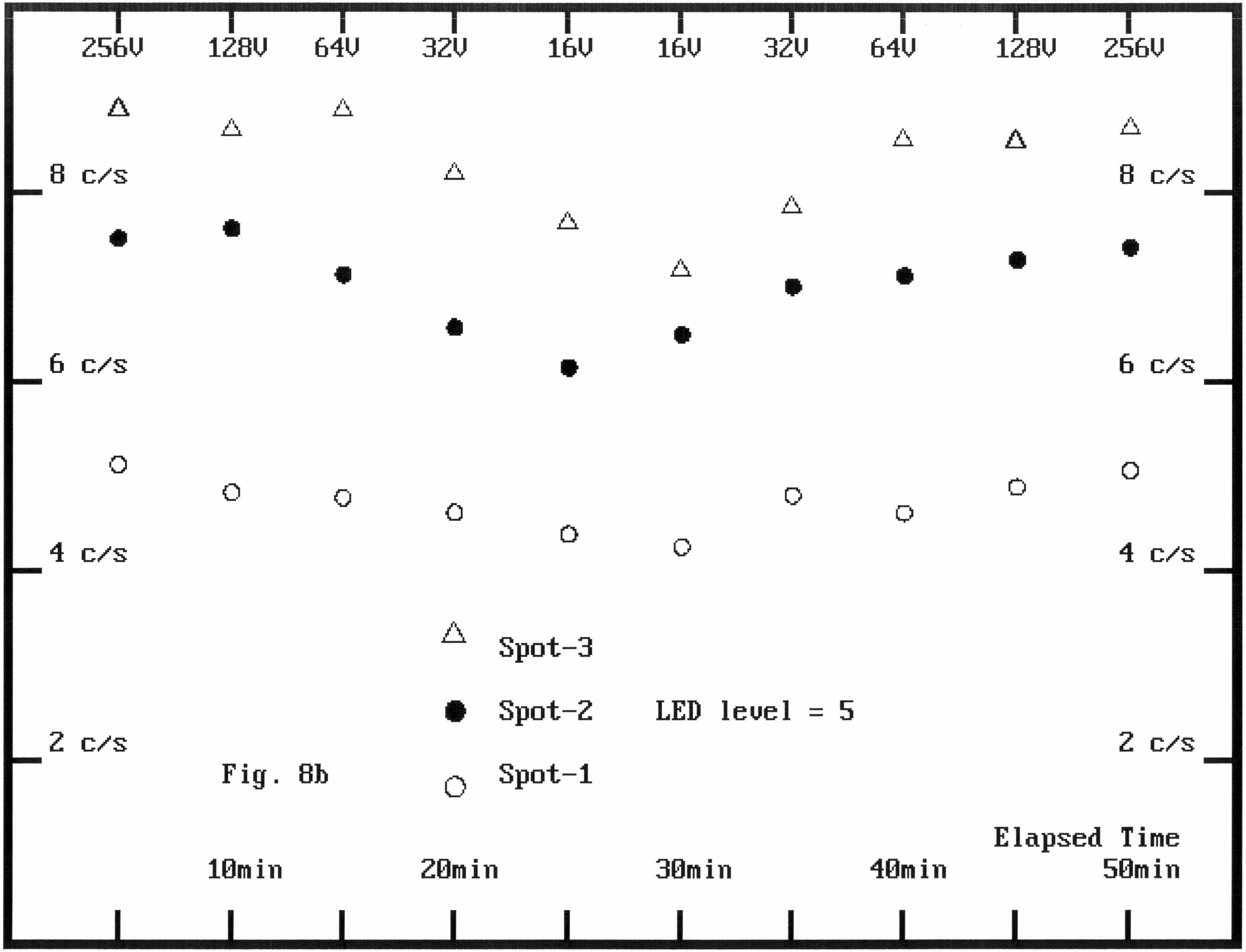
256V
128V
64V
32V
16V
16V
32V
64V
128V
256V
8 c/s
6 c/s
4 c/s
2 c/s
8 c/s
6 c/s
4 c/s
2 c/s
Spot-3
Spot-2
LED level = 5
Spot-1
Fig. 8b
Elapsed Time
10min
20min
30min
40min
50min

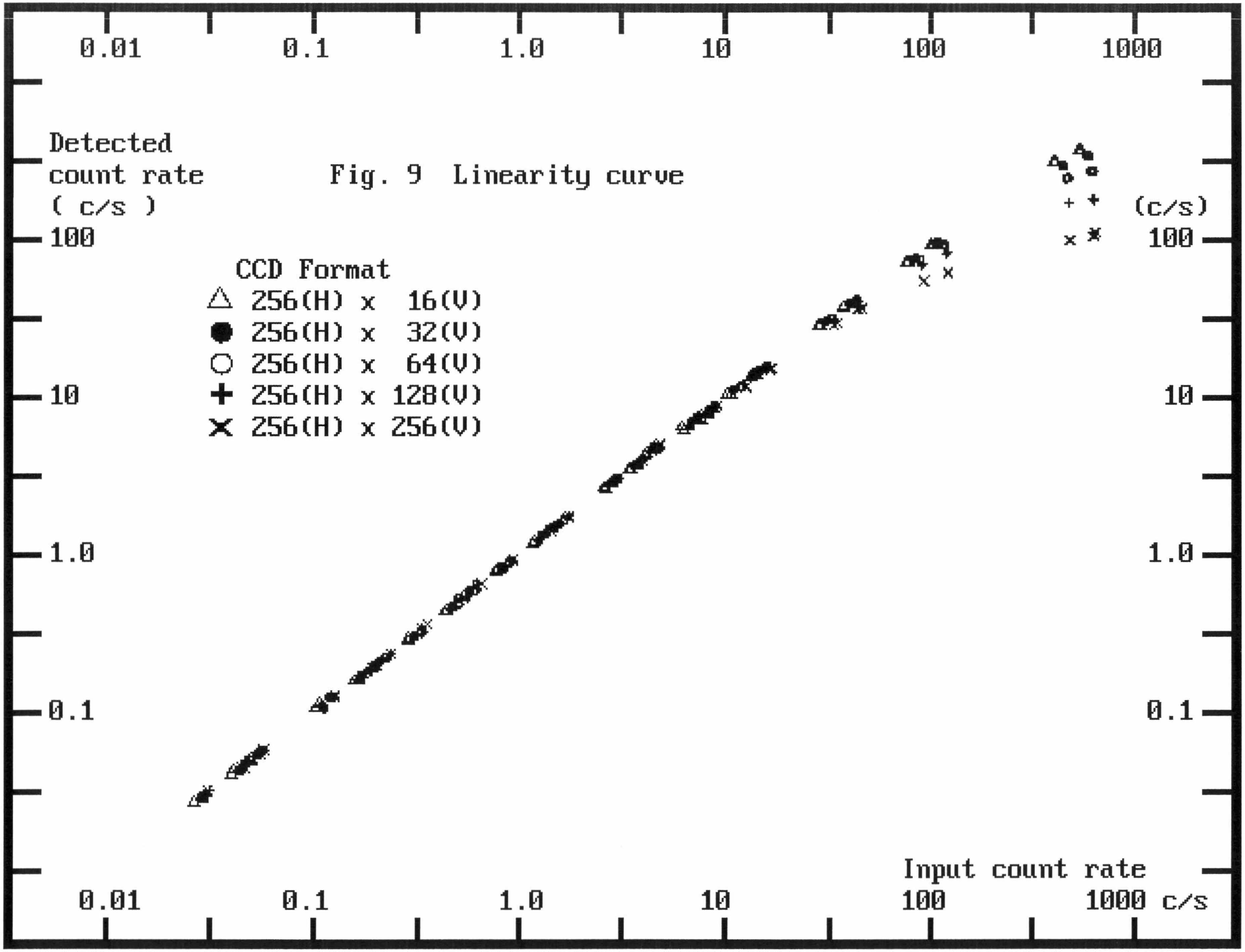

Fig. 9 Linearity curve

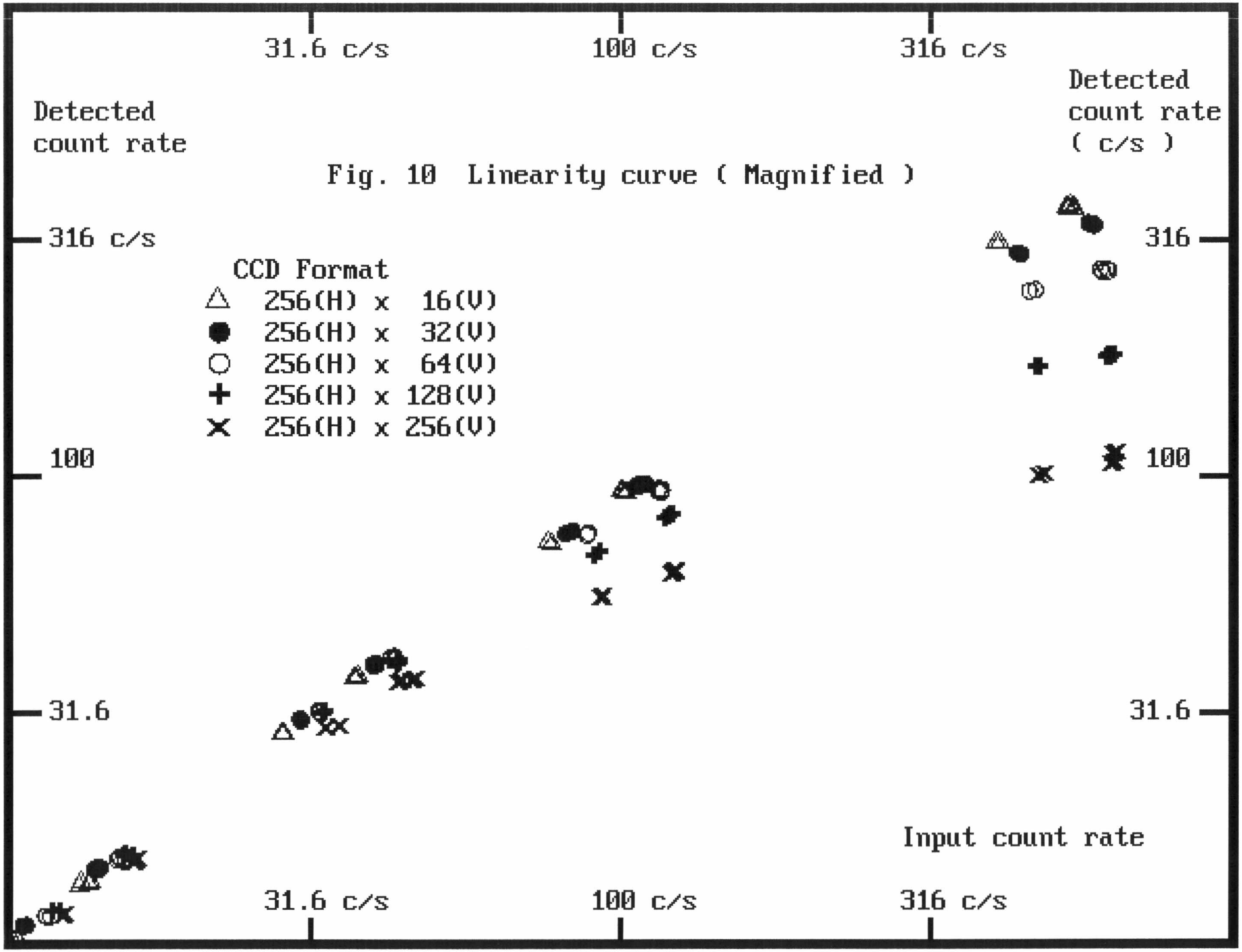
31.6 c/s
100 c/s
316 c/s
Detected
count rate
Detected
count rate
(c/s)
Fig. 10 Linearity curve (Magnified)
316 c/s
316
CCD Format
256(H) x 16(V)
256(H) x 32(V)
256(H) x 64(V)
256(H) x 128(V)
256(H) x 256(V)
100
100
31.6
31.6
Input count rate
31.6 c/s
100 c/s
316 c/s

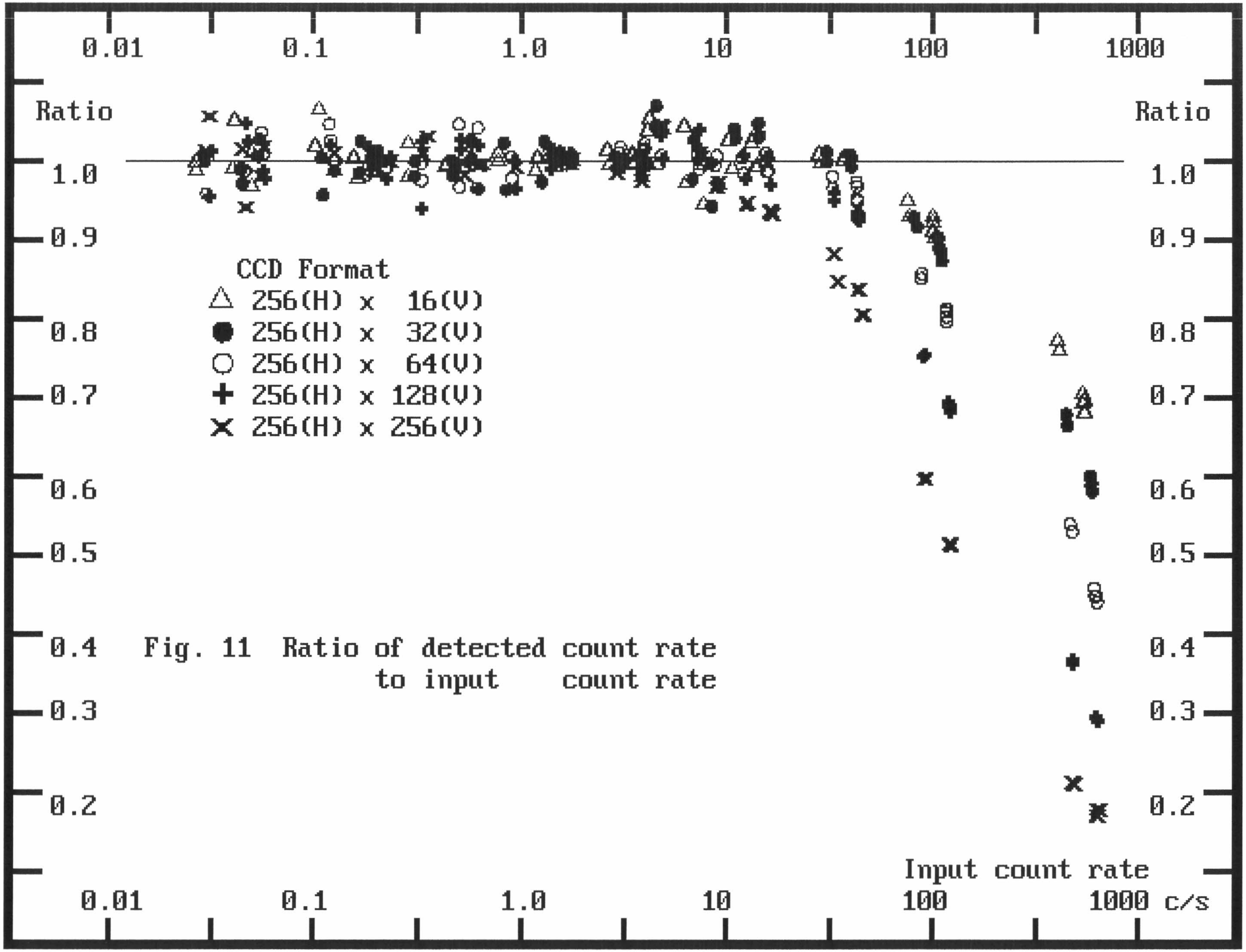

Fig. 11 Ratio of detected count rate to input count rate

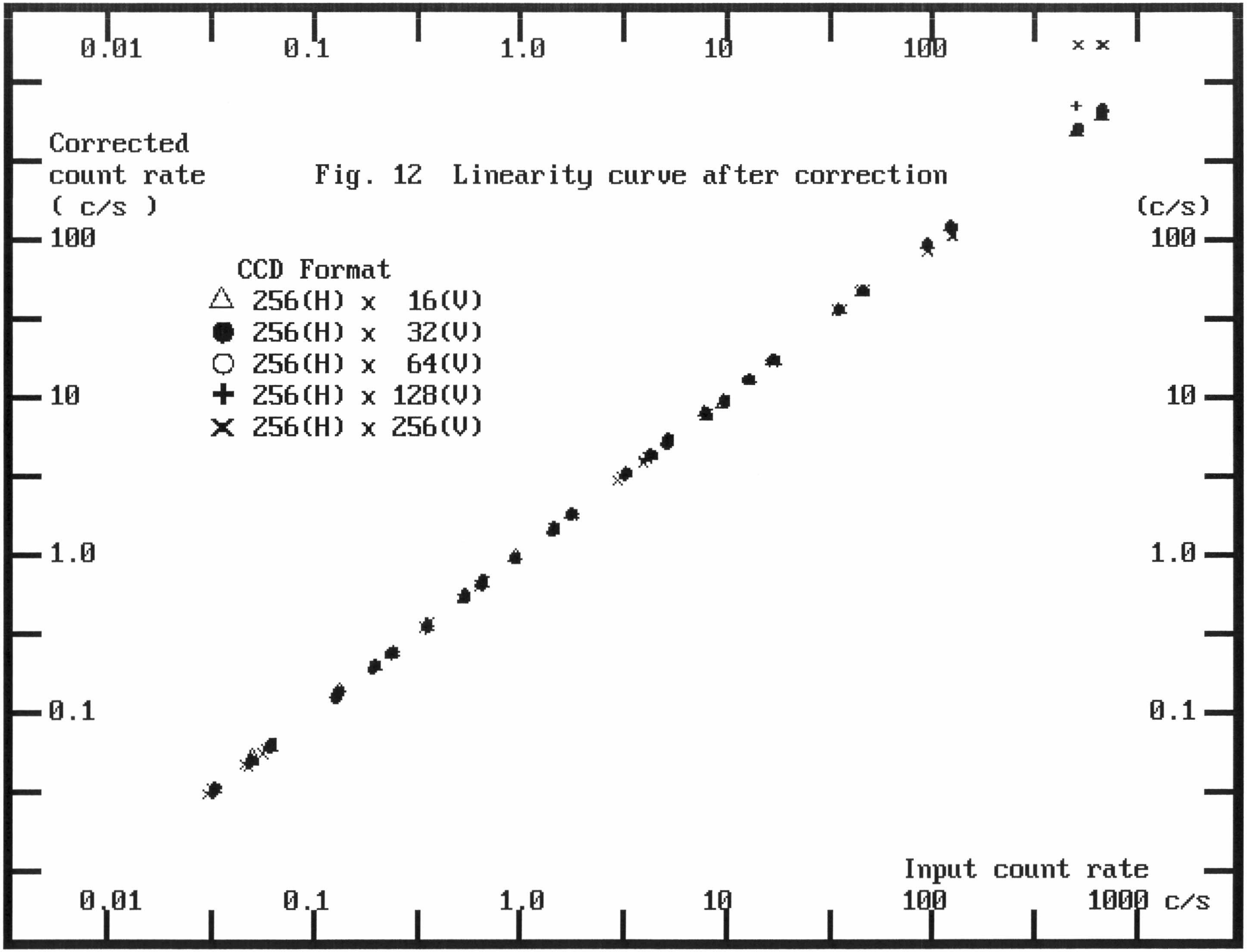

Fig. 12 Linearity curve after correction

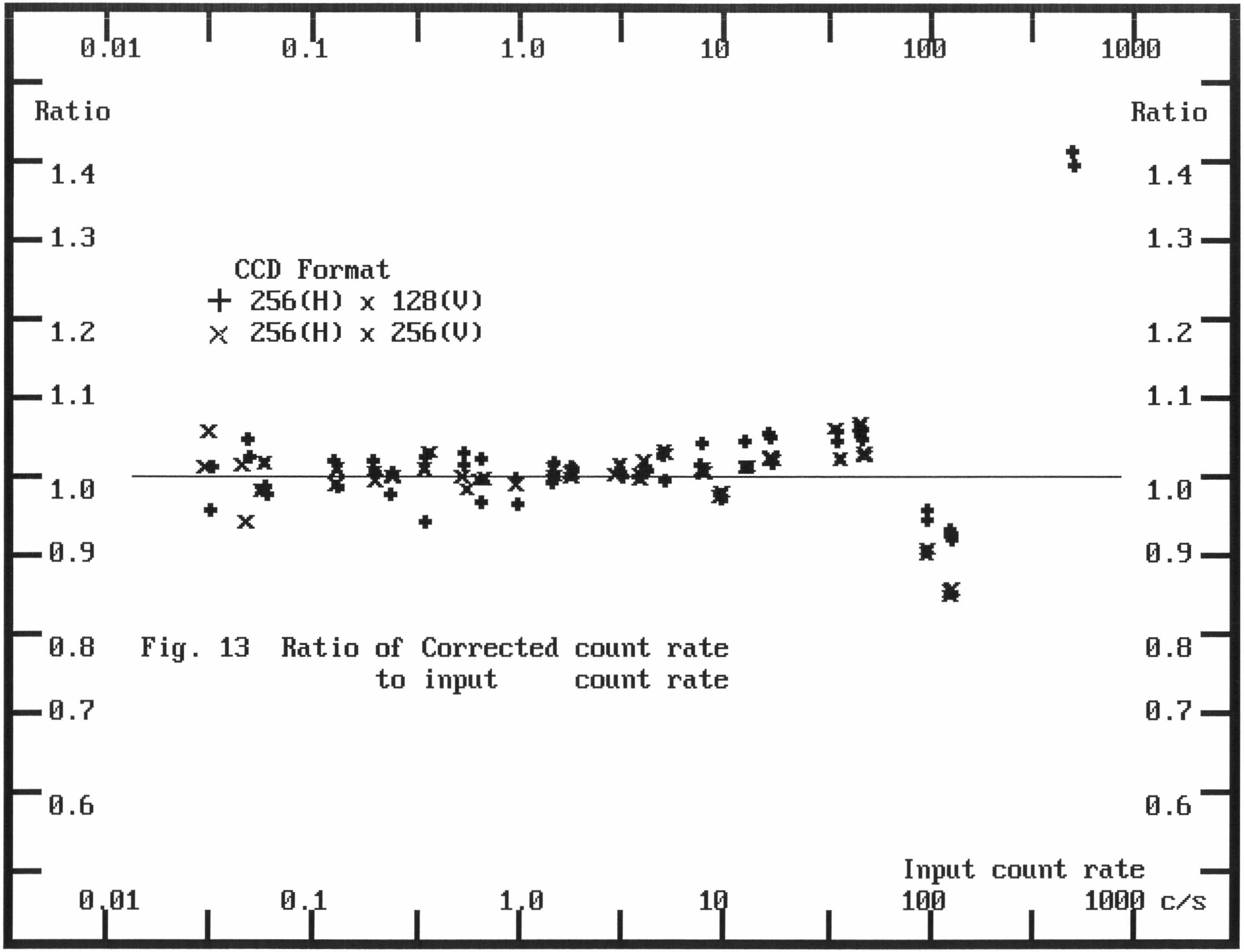

Fig. 13 Ratio of Corrected count rate to input count rate

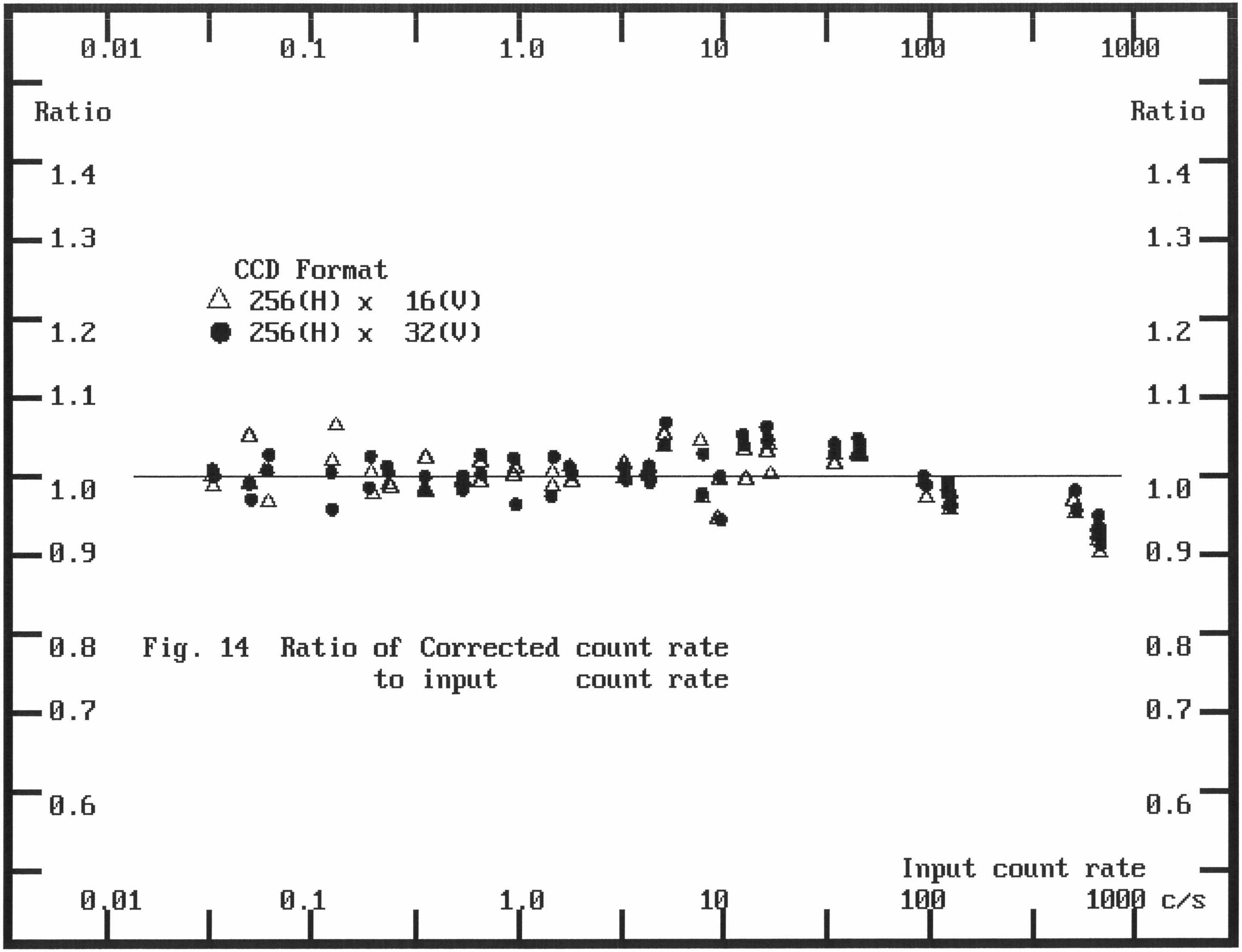

Fig. 14 Ratio of Corrected count rate to input count rate

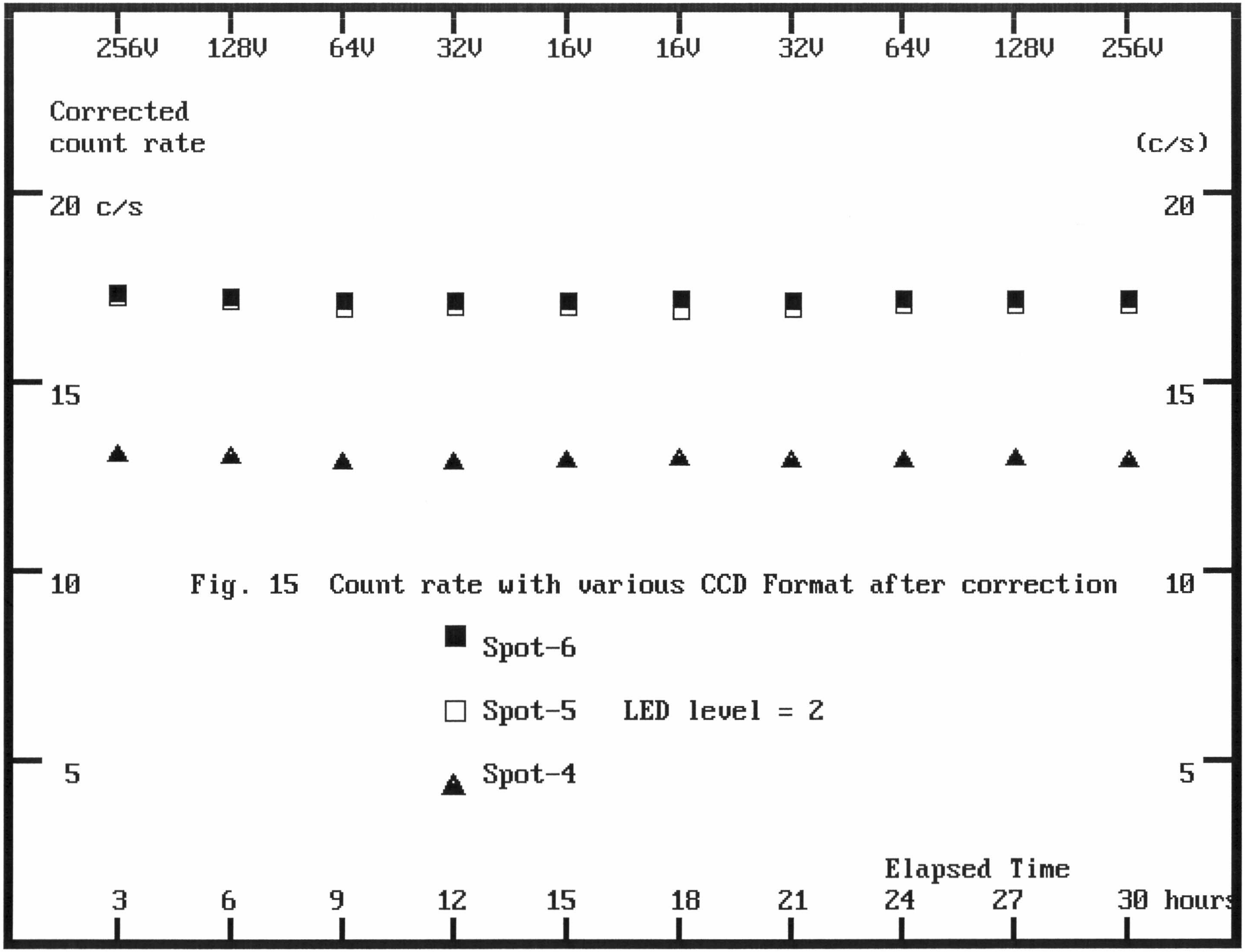

Fig. 15 Count rate with various CCD Format after correction

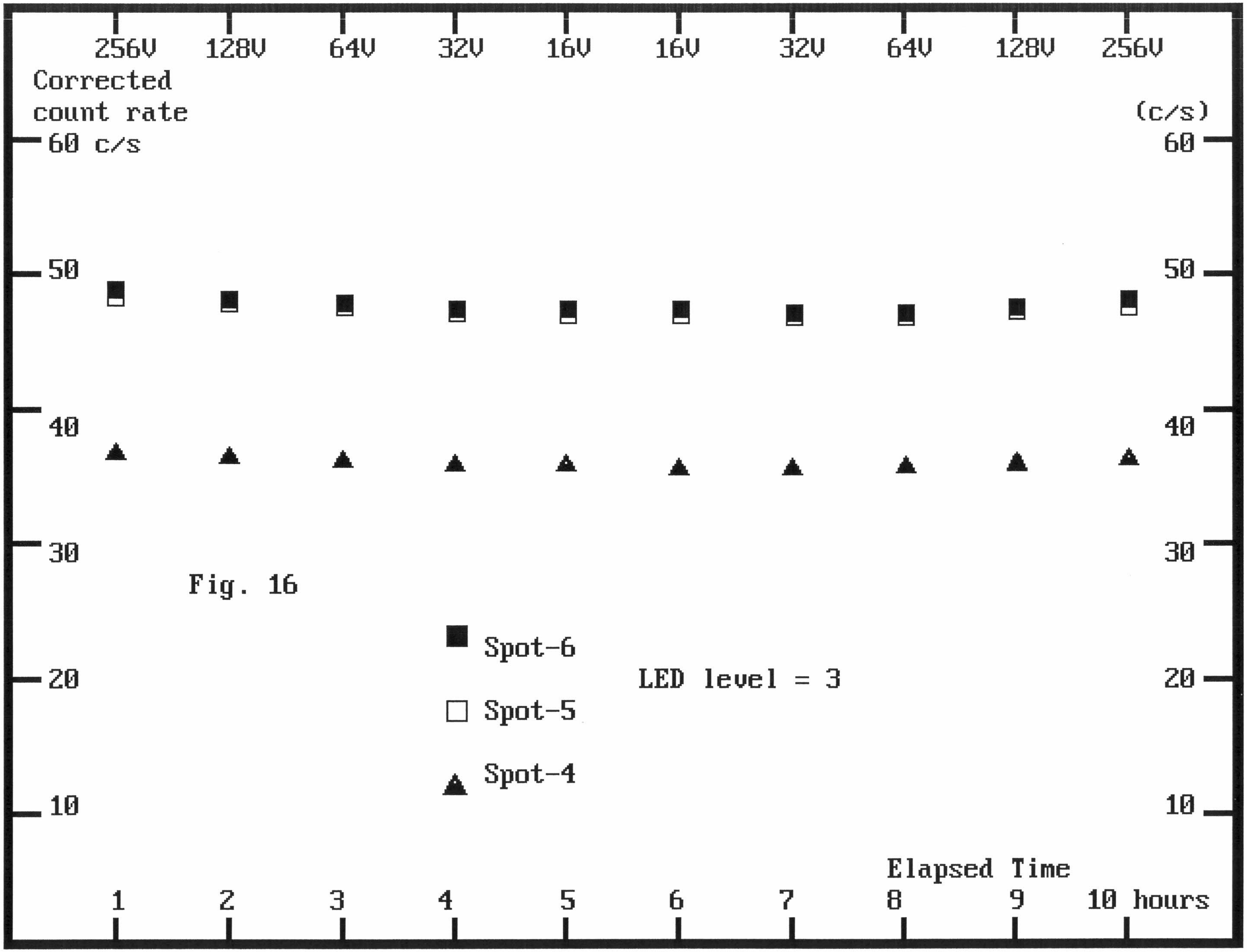
256V 128V 64V 32V 16V 16V 32V 64V 128V 256V
Corrected count rate
60 c/s
(c/s)
60
50
40
30
20
10
Fig. 16
Spot-6
Spot-5
Spot-4
LED level = 3
Elapsed Time
1 2 3 4 5 6 7 8 9 10 hours

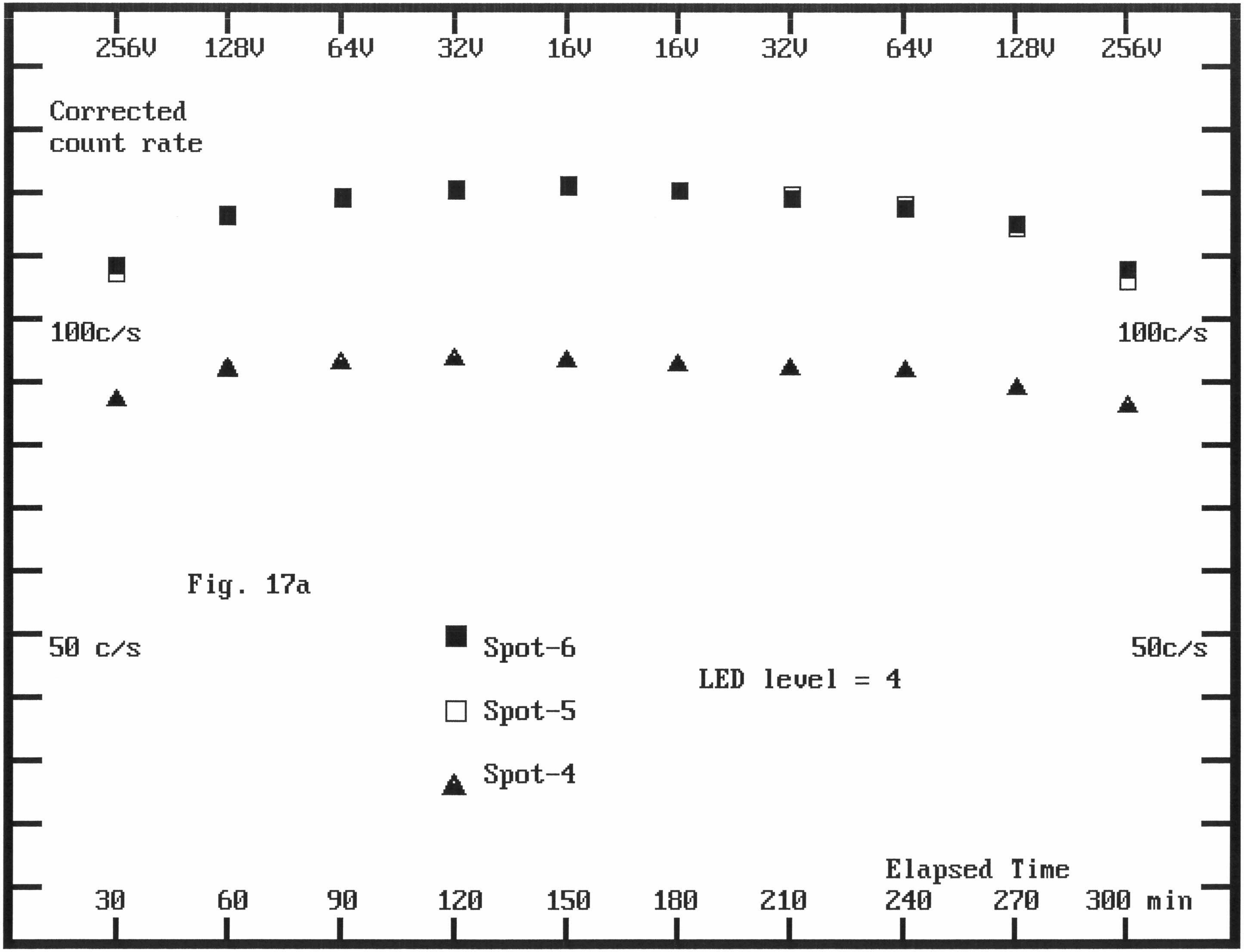
256V
128V
64V
32V
16V
16V
32V
64V
128V
256V
Corrected
count rate
100c/s
100c/s
Fig. 17a
50 c/s
50c/s
Spot-6
Spot-5
Spot-4
LED level = 4
Elapsed Time
30
60
90
120
150
180
210
240
270
300 min

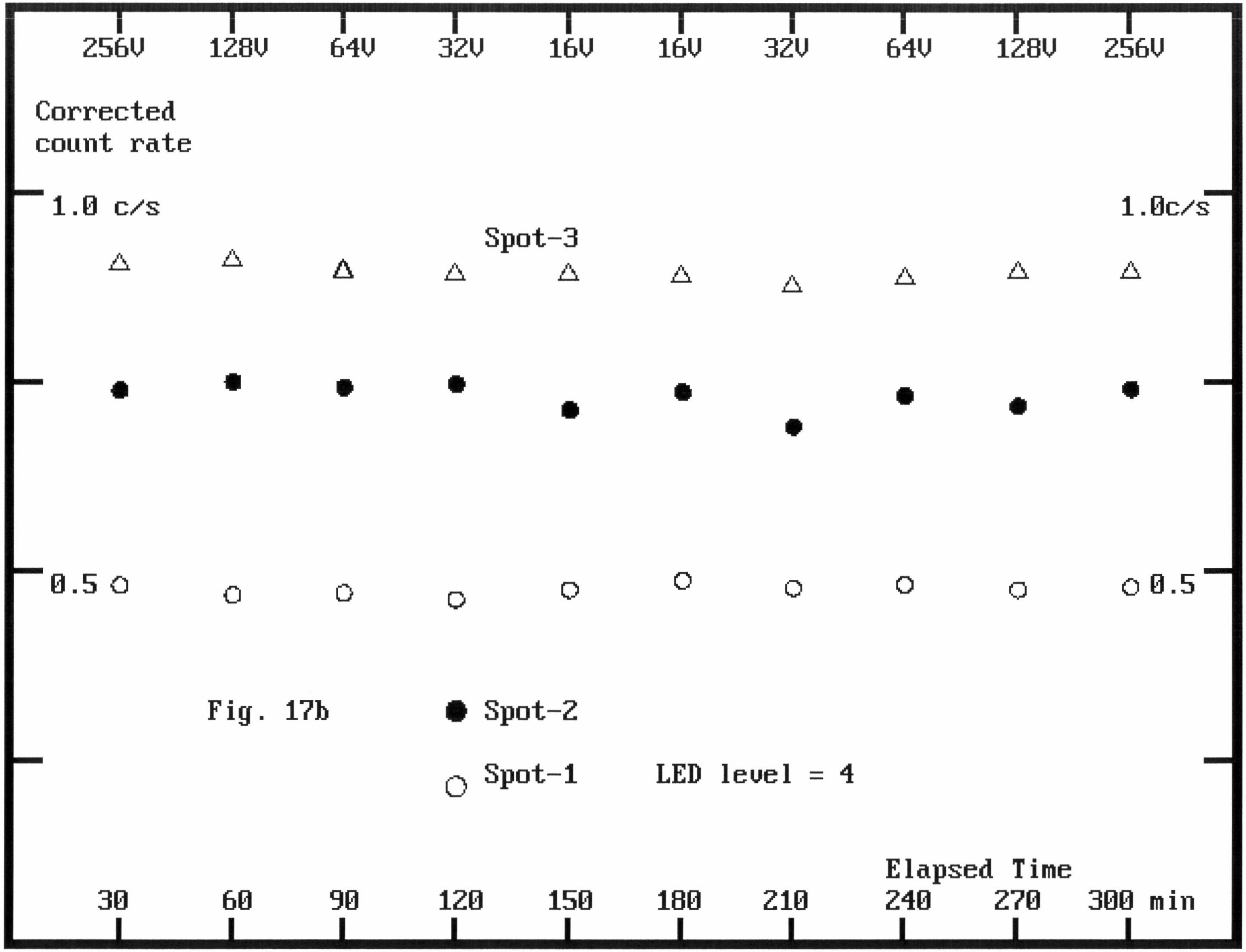

256V 128V 64V 32V 16V 16V 32V 64V 128V 256V
Corrected
count rate
1.0 c/s
1.0c/s
Spot-3
0.5
0.5
Fig. 17b
Spot-2
Spot-1
LED level = 4
Elapsed Time
30 60 90 120 150 180 210 240 270 300 min

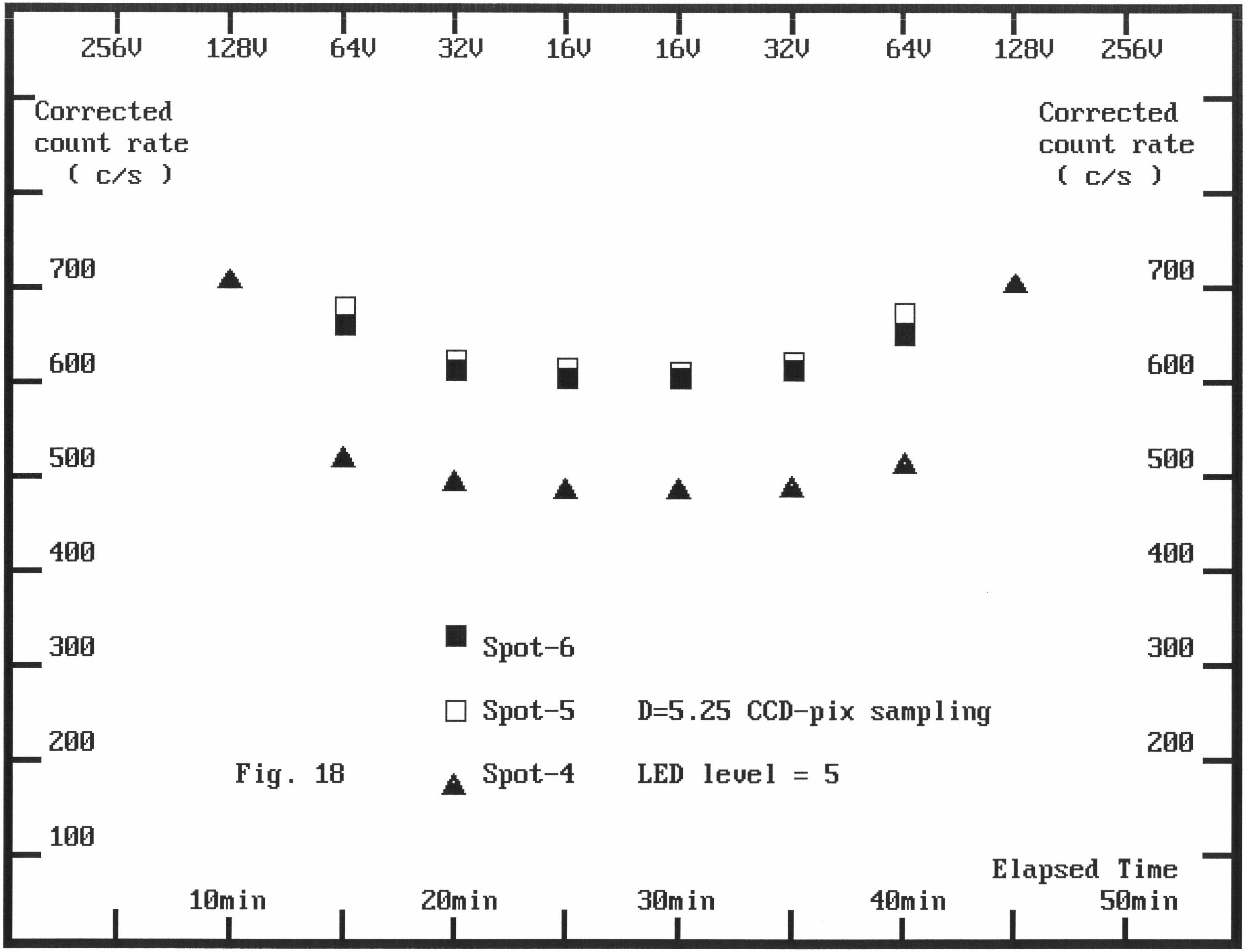
256V
128V
64V
32V
16V
16V
32V
64V
128V
256V
Corrected count rate (c/s)
Corrected count rate (c/s)
700
600
500
400
300
200
100
Spot-6
Spot-5
D=5.25 CCD-pix sampling
Spot-4
LED level = 5
Elapsed Time
10min
20min
30min
40min
50min
Fig. 18

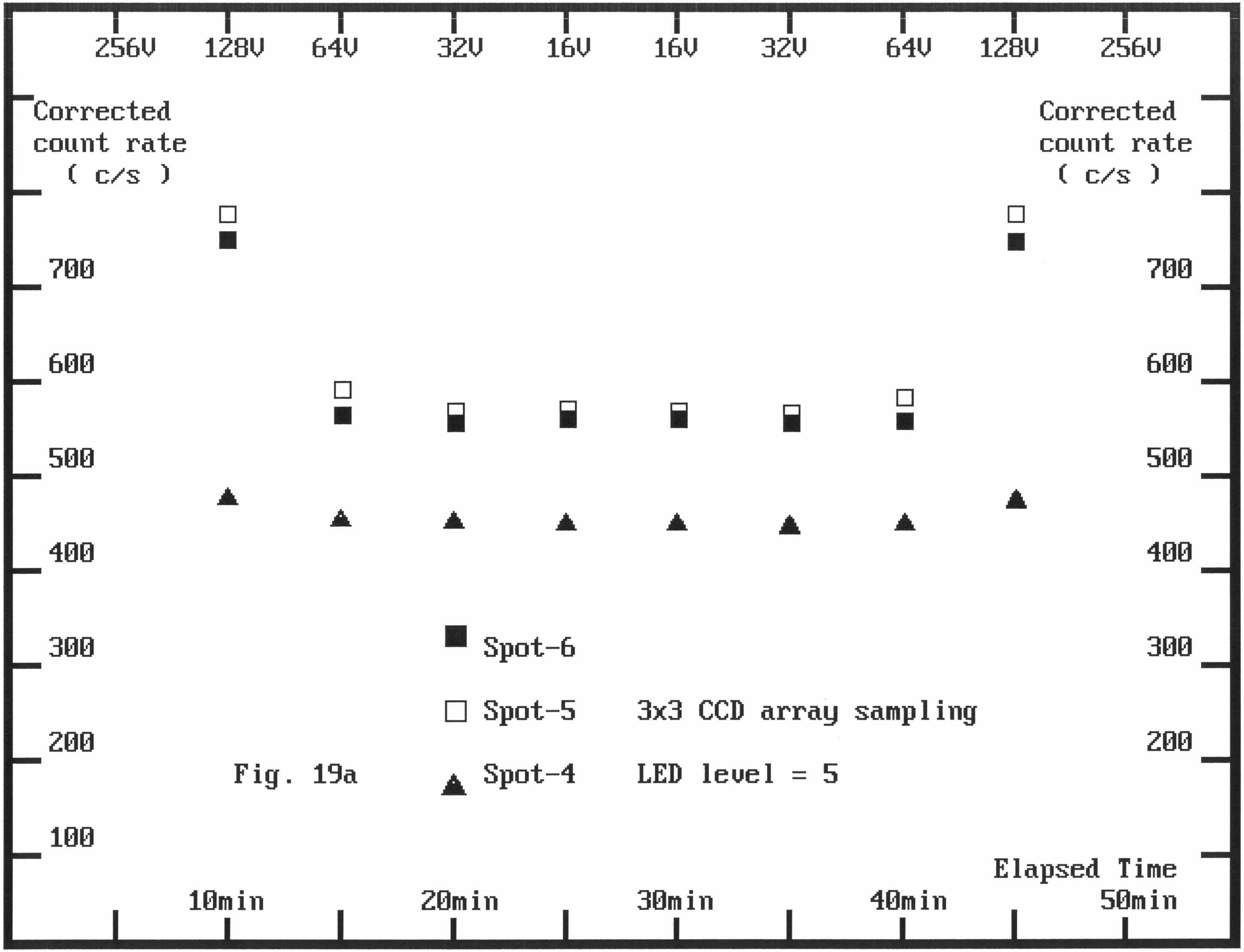
256V 128V 64V 32V 16V 16V 32V 64V 128V 256V
Corrected count rate (c/s)
Corrected count rate (c/s)
700
600
500
400
300
200
100
Spot-6
Spot-5
3x3 CCD array sampling
Spot-4
LED level = 5
Elapsed Time
10min
20min
30min
40min
50min
Fig. 19a

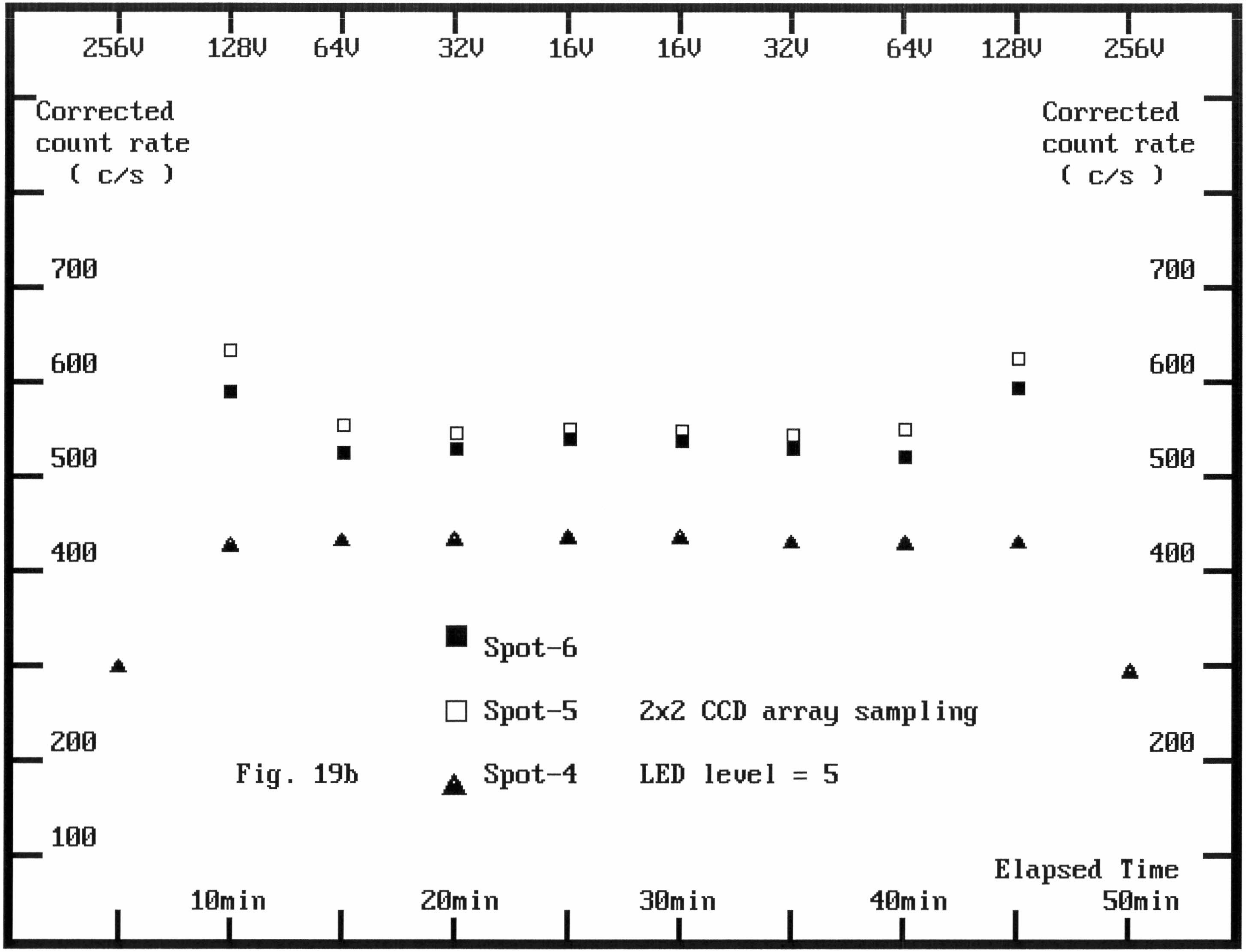
256V
128V
64V
32V
16V
16V
32V
64V
128V
256V
Corrected count rate (c/s)
Corrected count rate (c/s)
700
600
500
400
200
100
Spot-6
Spot-5
2x2 CCD array sampling
Fig. 19b
Spot-4
LED level = 5
Elapsed Time
10min
20min
30min
40min
50min

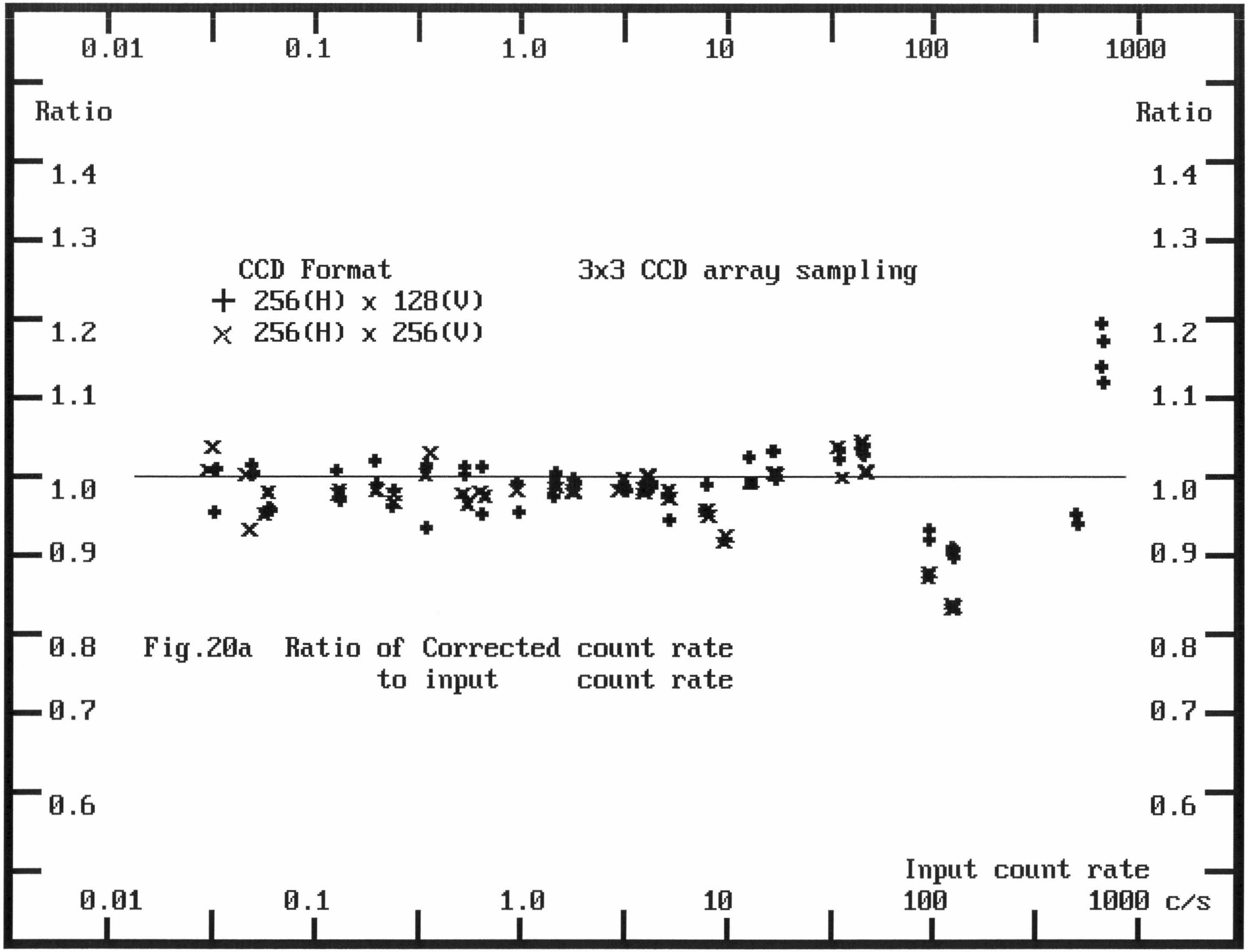

Fig.20a Ratio of Corrected count rate to input count rate

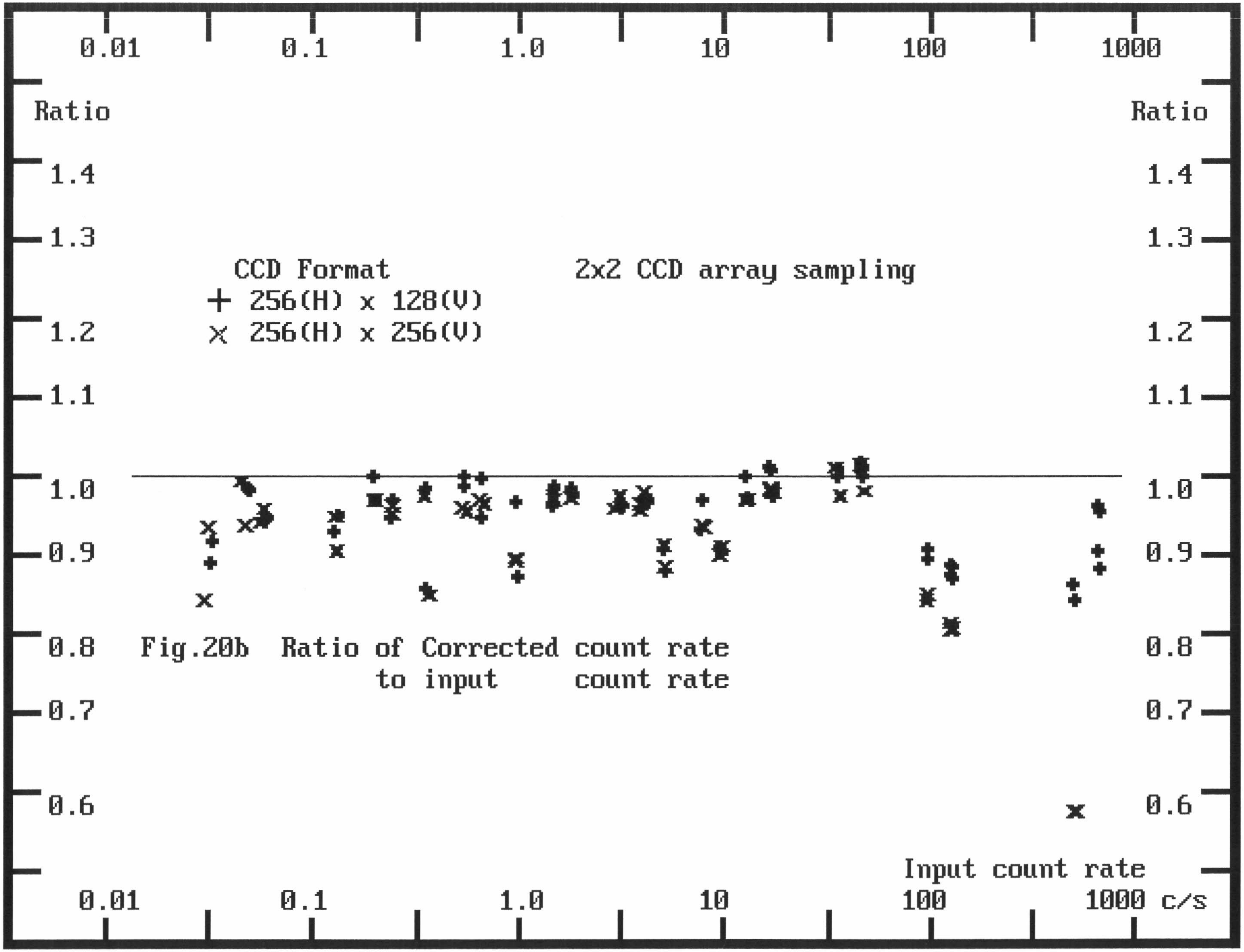

Fig.20b Ratio of Corrected count rate to input count rate